University of Baghdad
College of Engineering
Mechanical Engineering Department

AN ANALYSIS OF CRACKS IN SIMPLY SUPPORTED CURVED PLATES UNDER COMBINED BUCKLING AND IMPACT LOADING

ATHESIS SUBMITTED TO THE
COLLEGE OF ENGINEERING
UNIVERSITY OF BAGHDAD
IN PARTIAL FULFILMENT
OF THE REQUIREMENTS FOR
THE DEGREE OF MASTER
IN SCIENCE IN MECHANICAL ENGINEERING.

BY

JASIM HASAN ILIK

B.Sc July 1993

Supervisor/ Ass. Prof. Fathi A. AL-Shama'a

July 2009

بسم الله الرحمن الرحيم

﴿ اقرأ باسم ربك الذي خلق ۝١ خلق الإنسان

من علق ۝٢ اقرأ وربك الأكرم ۝٣ الذي

علم بالقلم ۝٤ علم الإنسان ما لم يعلم ۝٥ ﴾

صدق الله العلي العظيم

سورة العلق

الآيات (١-٥)

CERTIFICATE OF THE SUPERVISER

I certify that this thesis " **AN ANALYSIS OF CRACKS IN SIMPLY SUPPORTED CURVED PLATES UNDER COMBINED BUCKLING AND IMPACT LOADING**" was prepared under my supervision at the university of Baghdad in partial fulfillment of the requirements for the degree of master in mechanical engineering.

Signature ....

Name :Asst. Prof. Dr. Fathi A. S. Al-Shamaa

Date : 30/6 / 2009

CERTIFICATION OF THE EXAMINING COMMITTEE

We certify that we have read this thesis entitled "**AN ANALYSIS OF CRACKS IN SIMPLY SUPPORTED CURVED PLATES UNDER COMBINED BUCKLING AND IMPACT LOADING**" and as examining committee examined the student "**Jasim Hasan Ilik**" in its contents, and that in our opinion, it meets the standard of a thesis for the degree of **Master of Science in Mechanical Engineering.**

Signature:	Signature: Fathi Ahmed
Name: Prof. Dr. H.J. Mohamed Al-alkawi	Name: Asst. Prof. Dr. Fathi A. S. Al-Shama a
(Chairman)	(Member) Supervisor
Date: 28/ 7 / 2009	Date: 18/ 7 /2009

Signature: A. S. Al-Ammri	Signature:
Name: Ass. Prof. A. Salam Al-Ammri	Name:Dr. Widad I. Majeed
(Member)	(Member)
Date: 28/ 7 / 2009	Date: 20/ 7 /2009

Approved by the college of Engineering, University of Baghdad

Signature: K. M. Doos

Name: Prof. Dr. Qasim Mohammad Doos AL-Attaby

Date: 10 / 8 /2009

(Acting Dean of the college of Engineering)

DEDICATION

To my parents and my wife

To my son and daughter(Hassan &Ayaa)

To my brothers & sisters

To my teachers

To the poor who inherited me their rich

To everyone helped and supported me

Jasim H. Ilik

ACKNOWLEDGMENT

Thanks to god for all his blessings

I would like to express my thanks to my supervisor, **Ass. prof. Dr. Fathi A. S. Al-shamaa** for his valuable encouragement and fruitful discussion during the development of this work.

Special thank to **Eng. Amjed hameed** for his help and support during the present study.

I would like to thank the head , all staff members of mechanical engineering department at the university of Baghdad for their kind cooperation.

Jasim H. ilik

ABSTRACT

In this work a theoretical study the cracks in curved plates with mixed complex boundary conditions under in plane loading causes shear, compression and combined shear and compression buckling and low velocity impact at the edge of crack in the middle of simply supported curved plate .

Two methods of approximate analytical solution have been carried out for determining the critical loads and the stress distribution for curved plate which has two radius of curvature in xz and yz-planes with surface crack in the middle of the plate, the first one is derived from Airy stress function, equilibrium equations and large deflection plate theory to analyze the effect of different radii of curvature in two dimensions, buckling loads and duration time of low velocity impact loading on the stress distribution in plate with crack, the second method is derived from the energy method of curved plate which modified for including the impact loading with buckling loads and state the two dimensional stress for internal crack at the center of plate.

The stress intensity factors (SIFs), velocity of dynamic crack propagation with deep of crack normal to the crack face have been calculated, using the analytical method and a numerical package result (ANSYS-10), which based on finite elements method to investigate the stress and the values of dynamic stress intensity factor at the crack tip by full transient dynamic analysis in three dimensional element (Solid 20 nodes 95).

Two kind of materials are used in the theoretical analysis of the curved plates which are stainless steel and Aluminum.

The theoretical results have been verified with the experimental one that have been done by previous researches for curved panels without crack initiation.

The results for different aspect ratios (1:1 to 1:4) have been used, crack deep to crack length ratio (0.2- 0.8) under different impact velocities (5-30 m/s) gives good agreement with results of finite element analysis for long time duration in impact loading while the energy method is agreement with some values of time duration and then become limited when buckling occur.

The theoretical results obtained from classical and energy methods have deviation in the values of the principal stresses (σ_1 & σ_2), although the classical method gives good optimum results when compared with experimental one, the difference is at the range of (2.3 - 8.3 %) , and the percent of error in determining the dynamic stress intensity factor of the first mode (opening mode KI) when compare ANSYS-10 and classical method results has a percent of error less than that in determining the second mode (shear mode KII), the percentage of error in determining KI is about (0.3 – 3.2 %) but in determining the second mode KII the error is about (0.4 - 4.1 %).

The velocity of crack propagation in stainless steel panels greater than of Aluminum panels which have the same dimensions, location of crack and same loads applied so the steel panels have less safe than Aluminum panels under the same loading and boundary conditions.

Contents

Subjects page No.

List of tables

List of figures

List of symbols

Symbols	Meaning	Units
A	Length of the plate in x-direction	m
$\mathcal{A}$	Length of major axis of the elliptical patch.	m
a	Length of crack.	m
B	Length of the plate in y-direction	m
$\mathcal{B}$	Length of minor axis of the elliptical contact patch.	m
C_o	Depth of crack.	m
D	Flexural rigidity of a plate	N.m
DCG	Dynamic Crack Growth	m/s
E	Modulus of elasticity.	Mpa/m^2
H	The plate thickness.	m
K_b	Bending buckling stress parameter.	Unit less
K_s	Shear buckling stress parameter.	Unit less
K_{comb}	Buckling parameter for combined shear and direct compression.	Unit less
m_{im}	Mass of the impactor.	Kg
m & n	Number of half sine wave of the panel shape in y and x directions resp.	Unit less

Symbols	Meaning	Units
N_x	Direct compression/tension force in x-direction.	N/m
N_y	Direct compression/tension force in y-direction.	N/m
N_{xy}	Shear force in xy-plane.	N
p	The lateral force.	Pa
p_0	The maximum contact pressure (i.e. the pressure at the center of contact).	Pa
R_i	Radius of aspherical impactor.	m
r_c	Radius of patch due to impact.	m
s_{mn}	Lateral load mode shape due to impact.	Unit less
t_0	Time duration of contact.	S
v_{im}	Impact velocity.	m/s
w_c	Deflection due to direct compression only.	m
w_{ic}	Deflection due to impact and direct compression.	m
w_{ics}	Deflection due to impact, direct compression and shear.	m
w_{mn}	Mode shape of the deflection.	Unit less
w_o	The initial deflection.	M
w_s	Deflection due to shear only.	m
w_{sc}	Deflection due to shear and direct compression.	m
w_t	Total deflection.	M

Symbols	Meaning	Units
Z_p	Curvature parameter.	Unit less
α	The distance of approach of the impactor and the target.	m
α_{mn}	The maximum initial deflection at the center of the plate	m
$\dot{\alpha}$	The velocity of approach.	m/s
ß	Centric angle of the arc in yz plane.	rad
ξ	Coordinate of impact location in x-direction	m
η	Coordinate of impact location in x-direction	m
θ_p	Angle of principal stress.	Rad
μ	Poisons ratio.	*Unit less*
ρ_1	Radius of curvature in plane 1(i.e. curvature in xz plane).	m
ρ_2	Radius of curvature in plane 2(i.e. curvature in yz plane).	m
σ_{cr}	Critical bending buckling stress.	Pa
σ_x,σ_y&τ_{xy}	The Cartesian stresses.	Pa
σ_Y	The yield stress of the material	pa
σ_1&σ_2	The principal stresses.	Pa
τ_{cr}	Critical shear buckling stress.	Pa
Φ	Centric angle of the arc in that plane.	rad

Chapter one

Introduction

CHAPTER ONE

INTRODUCTION

When plates subjected to the application of large in-plane loads either compressive or shear they buckle .the phenomenon of buckling is actually a non-linear which is characterized by disproportionate increase of the displacements associated with the small increment of the loads; Buckling may be due to the action of the in-plane normal forces (N_x *or* N_y) along x or y direction respectively ,or due to the shear forces (N_{xy}) in the x-y plane. Either the previous forces acting individually or as a combination . Figure(1-1) shows the in-plane forces which can be applied, on the other hand, plates considered under large deflection develop internal resistive in-plane forces in addition to the transverse moments and shears, so plates do not fail under the critical load like columns**[1]**.

In addition to in-plane forces another forces out of this plane may apply such as impact forces in the direction normal to xy plane.

Failure does not take place by buckling only but also by fracture caused by crack growth.**[2]**

1.1 Buckling of Curved Plates

When plates subject to large in plane loads either compressive or shear ,they buckle. The buckling phenomena is not linear because it characterized by disproportional increase of the displacement associated with the small increment of the loads.

In plates ,buckling may occur due to the action of in-plane normal forces (N_x and N_y) along x or y direction respectively. or due to in-plane shear forces (N_{yx} and N_{xy}) in the x-y plane ,either acting individually or as a combination.

Unlike columns, the plate failure does not occur when the critical buckling load is reached .Plates continue to resist the in-plane loads far in excess to the critical load before failure ,thus the post buckling behavior of plates plays an important role in determining the ultimate carrying capacity **[3].**

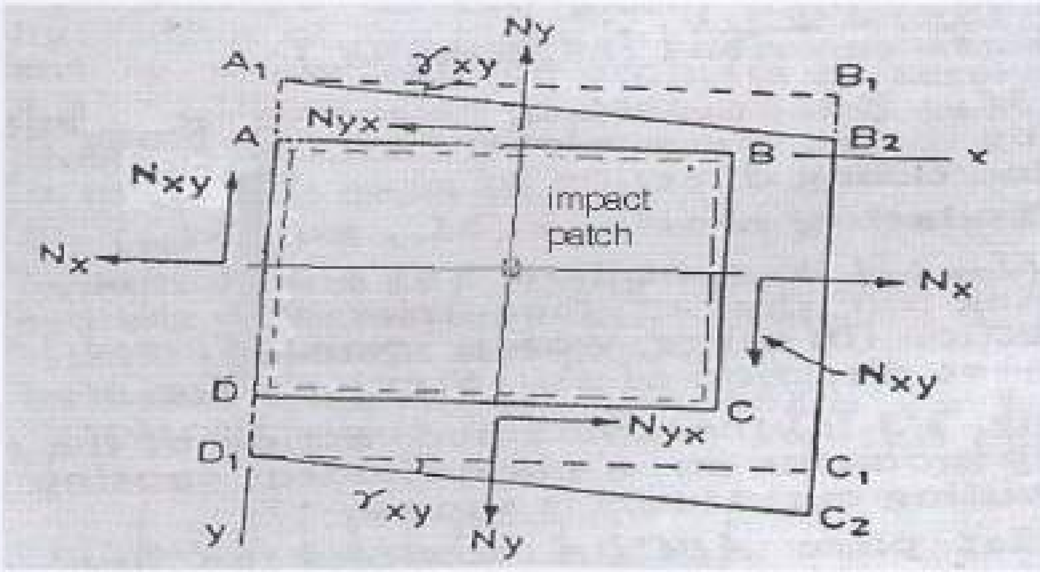

Figure(1-1) In plane forces act on plate.[1]

The failure of plates subjected to uniaxial compression may be due to instability or material failure. For thin plates (i.e. large values of *length to thickness* ratio) made from a typical strain hardening material with yield stress σ_y, instability occurs at an average stress σ_{cr} that is much less than the yield stress, especially if the plate has no crack in it. This stress is called *elastic* buckling stress. On the other hand, instability for relatively thick plates (i.e. low *length to thickness* ratio values), or plates with crack, may occur after the plate material has reached the yield point, or has passed it and entered the strain hardening stage at some portions of the plate, and that is called *inelastic* buckling. If the plate thickness is very large, material failure may occur before any buckling takes place.**[4]**

Flat and curved plates under combined shear and compression are structures commonly found in aero engine components such as vanes. In order to meet increasing demands to reduce the weight of such components, their thickness is constantly reduced, thus increasing the possibility of failure due to buckling.

Extensive work has been carried out to determine expressions for the critical buckling loads of such structures under the elementary load cases of shear, compression, bending and combinations of these three. These are based either on solution of the plate/panel differential equations for a particular set of load and boundary conditions, or the use of energy methods. However existing solutions are based on constant stress levels throughout the plate structure.

A few theoretical solutions or design rules exist for more complex solutions. Analysis is therefore based in practice on selecting the section of the structure considered to be most highly stressed, and assuming a simplified load case which can be solved.

In addition, only simple boundary conditions such as clamped or simply supported edges have been considered, with limited work being carried out on structures having combinations of the two. Due to these limitations, little confidence in calculated buckling loads exists and relatively high safety factors must therefore be incorporated to ensure collapse is avoided. Thus these techniques do not result in optimal designs. Finite element analysis has therefore been proposed as an alternative to theoretical techniques.

This has the advantage of being able to handle more complex geometries, boundary conditions and load cases. Two approaches are possible. A linear eigen value analysis can be carried out to determine the buckling load of a perfect structure.

Reduction factors can then be applied to account for the geometric imperfections and plasticity.**[5]**

For certain types of plate problems, on solving the governing differential equation of the plate satisfying the prescribed boundary conditions have been illustrated using classical method, Energy methods which are based on energy principles are often used as alternative solution methods for a large variety of plate problems .

Though approximate, the usefulness and efficiency of the energy methods can be particularly appreciated in problems which cannot be either solved by the rigorous classical methods or even if so , the procedure may often be too cumbrous and lengthy to be discarded.

When a plate element is acted on by external loads, the internal fibers of the material body absorb energy in the form of the *potential energy* and a result, the body shows deformed shape externally .On removal of the loads, the stored potential energy is converted to *Kinetic energy* so that the body wholly or partially regains its original position or shape. The absorbed potential energy of the internal forces stored within the structural body is often termed as *strain energy* (SE) or U, and its magnitude is equal to the work done due to the internal forces (in the opposite sense). The potential of the external forces V is defined as the work done by the external forces (in the opposite sense) during deformation between the initial and final position. The kinetic energy is the energy produced by the effect of the body, for example the vibration produced in a plate target under the action of impact hit.

1.2 Impact Loads on Plates

When an impactor hits a plate with a specific velocity there is a pressure produced in the target as well as the impactor, the distribution of this pressure depend on the velocity and shape of impactor and the mechanical properties of the target and impactor.

The approach in studying the response of the isotropic materials to low velocity impact is shown in figure(1-2) the three major steps of the approach are:

1. Determination of impactor-induced surface pressure and its distribution.

2. Determination of internal stresses in the target caused by surface pressure.
3. Determination of failure modes in the target caused by surface pressure.

There are other assumptions will be considered for the case of study as will be noticed in chapter three of this study.

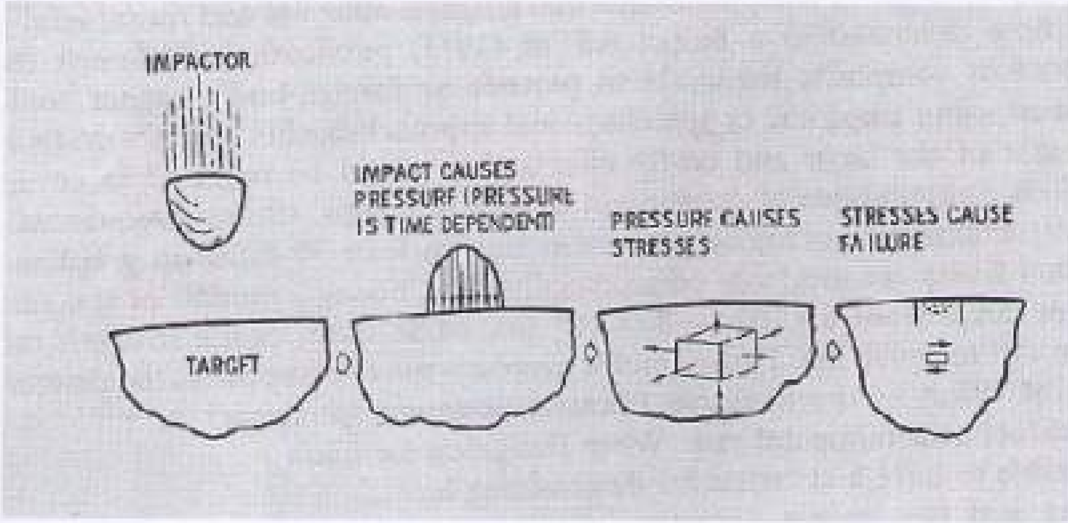

Figure(1-2) Essential features of the approach.[6]

1.3 Crack Modes

According to the loading condition there are three crack modes as shown in figure (1-3).

These modes always designated by roman numbers I, II and III. The first is the opening mode or tension mode ,the second is shearing (in-plane) mode , while the third mode is tearing mode (i.e. out of plane shear mode).

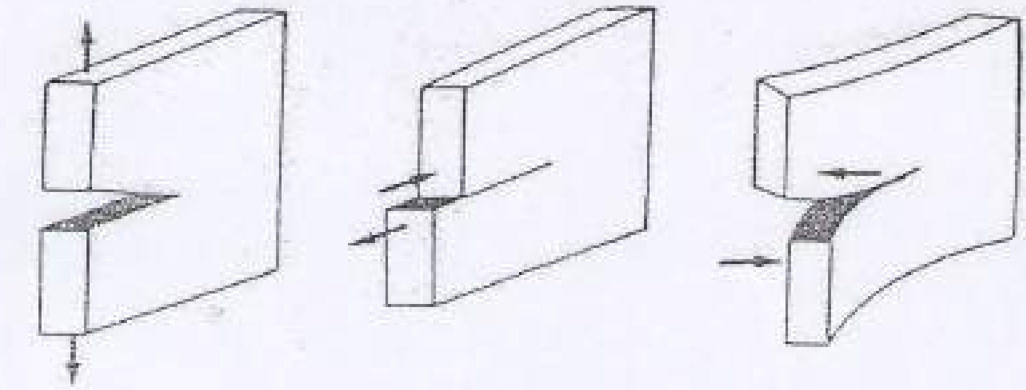

Figure (1-3) Modes of loading[7].

In practical cases the majority of cracks result from loading mode I. The others do not occur individually ,but they may occur in combination with mode I , i.e. I-II, I-III or I-II-III.

If the loading of these modes is in phase , crack will rapidly choose a direction of growth in which they subjected to mode I only. Thus the majority of apparent combined mode cases are reduced to mode I by nature itself.

1.4 Dynamic Crack Growth(DCG)

The Dynamic Crack Growth(DCG) in Structure is divided into:-

• *Static growth*, this state happens in equilibrium condition of crack propagation , this growth take long time so it consider stable growth also it has been effected by the temperature of the surrounding, this type of growth can be controlled easily ,and the researches dealt with it at the beginning stage , as example of this type of growth is that which take place due to creep loads.

•*Quasi-static growth*, this state happens without kinetic-energy production, the potential energy will gradually approach zero since the fractured pieces obviously are free of stress as the state of elastic loads.

The time of this growth is longer than that of static growth and the temperature has less effect. There are many examples of this type of growth such as low velocity impact loading, sustained loads on cracked structures....etc

•*Dynamic growth*, this state happens with kinetic-energy production. The crack driving force in this state is large than that in quasi-static growth, also it is difficult to controlled for example of this growth the fatigue crack growth.

1.5 Objective of this Work

The objective of this work is to study the three dimensional crack problems of curved panels under the action of direct compression, shear and low velocity impact loading to evaluate the dynamic crack growth using classical theory of plates, and energy method then resolve the problem with numerical method using finite element analysis to compare the results achieved.

To achieve the above objective the following steps are followed:

1. This thesis studies analytically the propagation of crack in curved plates under the action of direct compression, shear and low velocity impact loading using equilibrium equations (i.e. classical theory of plates).
2. Strain energy method of solution have been used also in the analytical solution to support the results of step 1, using plane stress case of analysis.
3. Using numerical computer software (ANSYS-10) based on the finite element method to calculate the stress intensity factors, these results are compared with the analytical solution in steps 1 & 2.
4. The above calculation have been made for different low velocities of impact (5-30 m/s),depth of crack, thickness of panel, radius of curvature of the curved panel and the properties of plate material. The results show the effect of these parameters on the stresses and stress intensity factors then

on dynamic crack growth when the curved plate subjected to low velocity impact by spherical steel impactor.

1.6 Layout of Thesis

In order to achieve the objectives mentioned above , the current chapters are arranged as follows:

Chapter two present the review of the previous studies which deals with buckling, impact, dynamic crack growth and curvature effect.

Chapter three contain the theoretical analysis for direct compression, shear and impact loading (classical method) on plates without crack to check the derivation of the equations by making a comparison with the values achieved experimentally by Featherstone(1998) then solving the same problem using energy method to get the stresses and dynamic crack growth.

Chapter four contain the finite element method nodal analysis as well as the build of cracked panel nodes and elements using MACRO steps in ANSYS-10 program (see Appendix C) to know how built the nodes and the elements of this case study. This chapter also contain the steps of acting the loads and the method of getting pictures and movies during the solution.

Chapter five contain results, discussion and comparison of the results achieved by classical, energy and numerical methods of solution.

Chapter six present conclusion and recommendations for future work.

Chapter two

Literature Survey

CHAPTER TWO

LITERATURE SURVEY

2.1 Introduction

Studies of buckling and fracture mechanics are very widely reported. In this chapter, the literature on buckling, impact, and dynamic crack growth will be considered .

2.2 Buckling of flat and curved plates:

There are two types of buckling (bending and shear)some scientists studied the combined buckling of these two types of loading together on plates.

(1) W. Jefferson Stroud et al [8](1984), examined several buckling analysis procedures for stiffened panels, they presents accurate results for seven stiffened panels and illustrates buckling modes with plot of buckling mode shapes. All panels are rectangular and have stiffeners in one direction down the length of the panel. PASCO buckling analysis include the basic VIPASA analysis which is essentially exact for longitudinal and transverse loads, and a smeared stiffeners solution(equivalent orthotropic plate solution) that was added in an attempt to alleviate a shortcoming in the VIPASA analysis-underestimation of the shear buckling load for modes having a buckling half-wavelength equal to the panel length.

The EAL and STAGS solutions where obtained with a fine finite element mesh and are very accurate.

(2) C A Featherstone And C Ruiz [9],*(1997)*, made analytical work to determine the buckling load and post buckling behavior of curved panels under various types of loading and different boundary conditions not as comprehensive as that for flat plates. Only elementary loading and boundary conditions have been analyzed .In addition to this, many of the theories developed have not been tested experimentally. Their study outlines a series of tests carried out to determine the accuracy of the theoretical and numerical buckling loads. The experimental results were used to examine whether or not finite element analysis can be used as an alternative to determine collapse loads and post buckling behavior, especially in cases where no theoretical solution exist.

they show that, existing analytical techniques can be used to determine buckling loads for a structure such as curved panel under the complex loading case of compression and shear this is done by selecting the most highly stressed section of the panel, simplifying both the load case and the boundary conditions and using set formulae. It is concluded that Designers should be advised to follow simple analytical results to produce a preliminary design and finite element analysis should be limited for checking its adequacy.

***(3) C A Featherstone And C Ruiz* [10],*(1998*)**, determined an expression for the critical buckling loads of plates under elementary load cases of shear ,compression ,and bending ,and combination of these three are achieved .Collapse load predicted by theoretical ,experimental and numerical (using finite element analysis) for rectangular flat plates under combined shear and bending loads with different boundary conditions have been studied. They conclude that

1. Application of existing theoretical solutions to the problem of shear loading in rectangular plates caused by a force applied across one end results in an underestimation of the buckling load.
2. The boundary conditions of a plate loaded in shear and bending , particularly at the edge to which the force applied, are important in calculating the critical load for all aspect ratios.

3. The buckling of a plate under shear and bending is sensitive to imperfections such as misalignment and curvature of the plate.
4. Finite element analysis can be used to provide better limits for the buckling load of a plate due to improved modeling of boundary conditions and distributed stresses.
5. Finite element analysis is still not able to handle more complicated boundary conditions.
6. Eigen value analysis can only be used providing buckling occurs within the elastic region.

***(4) C.A. Featherstone et al (2000)*[5]**, the use of finite element buckling analysis in the stability design of thin shelled structures allows complex geometries and load and boundary conditions been considered. Two approaches are possible. A linear bifurcation buckling analysis were carried out to determine the bifurcation load of the perfect structure. Reduction factor then been applied to account for the geometric imperfections and plasticity. Alternatively a fully non-linear analysis can be performed with deflections, geometric imperfections and plasticity properly modeled. Their work assesses the suitability of each of these methods to predict the buckling loads and post-buckling behavior of two structures flat plates and curved panels under combined shear and compression a load case commonly found in aero engine structures such as vanes. Experimental data is also presented for comparison.

(5) Khaled M. El-Sawy and Aly S. Nazmy*[4] *(July 2001), employed Finite Element Method (FEM) to determine the elastic buckling load of uniaxial loaded rectangular perforated plates with length a and width b. Plates with simply supported edges, in the out-of-plane direction and subjected to uniaxial end compression in their longitudinal direction are considered.

Integer plate aspect ratios, A/B=1, 2, 3 and 4, have been chosen to assess the effect of aspect ratio on the plate buckling load.

Two perforation shapes of different sizes are considered; circular, and rectangular with curved corners. The rectangular perforation is oriented such that either its long or its short side is parallel to the longitudinal direction of the plate. The center of perforation was chosen at different locations of the plate. The study shows that the buckling load of a rectangular perforated plate that could be divided into equal square panels is not the same as that of the square panel that contains the perforation when treated as a separate square plate. For rectangular plates, the study recommends not to have the center of a circular hole placed in a critical zone defined by the end half of the outer square panel, to try always to put the hole in an interior panel of the plate, and to have the distance between the edge of a circular hole and the nearest unloaded edge of the plate not less than 0.1 of the panel length. The study concludes also that the use of a rectangular hole, with curved corners, with its short dimension positioned along the longitudinal direction of the plate is a better option than using a circular hole, from the plate stability point of view.

(6) Cairns et al.(2005) **[11]**, presented an analytical solution for an orthotropic plate subjected to general lateral loading. The results showed that the analysis agrees well with the experimental data and could be used in conjunction with failure criteria to predict damage initiation in a localized region. The composite materials have high strength-to-weight and high stiffness-to-weight ratios. However, they are susceptible to impact loading because they are laminar systems with weak interfaces. Matrix cracking and delamination are the most common damage mechanisms of low velocity impact and is dependant on each other. In fact delaminations are generated by matrix cracks, which are the initial damage. In the presence of delaminations, the stiffness of the material and thus of the associated structure may be significantly reduced, which may result in a catastrophic failure of the structure. It is therefore highly desirable to estimate the delaminations in the composite materials, submitted to impact loading.

Many researchers have made effort to analyze the impact behavior of composite structures. However, only some studies have so far been devoted to the damage prediction of low velocity impact on composite laminates.

(7) I. Shufrin, O. Rabinovitch & M. Eisenberger (may 2008) **[12],** presented semi-analytical approach to the buckling analysis of generally supported laminated plates subjected to a general combination of in-plane shear, compression, and tension loads.

Arbitrary out of plane and in-plane boundary conditions at the edges of the plate are considered. The formulation is based on the variational principle of virtual work and the multi-term extended Kantorovich method. The semi-analytical method is used for the pre-buckling and buckling (stability) analyses of laminated rectangular plates with in-plane restraints under arbitrary in-plane loads. The accuracy and convergence are examined through a comparison with exact solutions (where available) and with finite element analyses. The applicability of the method is demonstrated through various numerical examples that focus on the buckling of rectangular composite plates with a variety of boundary conditions and various combinations of the in-plane shear, compressive, and tensile loads.

2-3 Impact Loading and Time Duration

The classification of impact loading is according to the velocity of the impactor and the literature survey concentrate on low velocity type which is in the scope of this study.

(1) Longin B. Greszczuk (1981) **[13],** obtained the magnitude and distribution of surface pressure in the target caused by impact can be obtained by analytically combining the dynamic solution to the problem of impact of solids with the static solution for the pressure between two bodies in contact ,similar to the method described by Timoshenko (1934)for impact of spheres.

He conclude the following

1. Resistance to damage increase as the fiber strength increases and the fiber modulus decreases.
2. Resistance to damage increase as the young's modulus of the matrix decreases and the strength of the matrix increases.
3. Bidirectional layup is more efficient in resisting damage than tridirectional or unidirectional layup.
4. Impact can cause extensive internal damage with very little or no visible damage on the outer surface.
5. Target curvature effects the impact parameters and failure modes.

***(2) Vijay Maka and M. A. Wahab (2005)* [14],** represented analytical study of damage response due to impact load on composite plates, they noted the various parameters like fiber orientation, fiber thickness, mass of impactor, velocity of impactor, and boundary conditions are vary effective on damage initiation and propagation.

***(3) Arman Murad (2006)* [15]**, presented analytical study for calculating the stress intensity factors in cracked plates under combined (buckling and tension) loads and impact loading (static load as Hertzian contact) for different aspect ratios, and crack angle, by using Lagrange equation. The analytical results compared with the numerical results using ANSYS-9.0 program.

A 3-dimensional finite element analysis and 2-dimensional analysis for stress intensity factors (SIFs) (KI and KII) in isotropic plates was performed St.steel and Aluminum plates with different aspect ratios and crack angles were considered under combined (buckling and tension) loads which were applied to the edges of the plate. Numerical and analytical results of (KI & KII) had been compared .

***(4) Ali Fahad Fahem (2007)* [16],** the effect of impact loading on dynamic crack propagation in thin and thick isotropic plates are investigated analytically and numerically to give a study of 3-D crack growth. The stresses are computed using classical and energy methods . The dynamic stress intensity factors have been obtained at different time of impact duration under impact velocity(2-8 m/s), the crack opening displacement and crack propagation using Dugdale theory for plane stress and plane strain are investigated.

The major observation and conclusion from study dynamic analysis, simply supported stainless steel and aluminum cracked plated, under various impact velocities by cylindrical steel are listed as follow:

1. The results of DSIFs and velocity of crack propagation obtained by the building of programs by FORTRAN bower station-90, for impact loading. These results have been obtained by two different ways. First by using classical method, and secondly by energy method. These two ways is gives the some results with percentage error is lowest than (15%).
2. In the case of internal crack the values of dynamic stress intensity factors (DSIFs), is depended on the depth of crack and angle of local (alpha).
3. The duration of time impact is decreasing when the velocity of impact is increasing, and when the young modulus is increasing the duration time decreasing i.e. the duration of time depended on the properties of material.
4. The crack propagation activity at location when maximum DSIFs along the crack front. Also the plastic area is large then compared with a critical plastic area (Dugdal model).
5. The velocity of crack propagation in steel is larger than that in aluminum because the difference in young modulus.

6. The velocity of crack propagation in plain stress is larger then in plain strain, i.e. the crack velocity is decreasing when thickness of plates is increasing.
7. The velocity of crack propagation is decreasing when the aspect ratio is increasing. In addition, increasing velocity of crack when velocity impact increase, when deep of crack increase the crack velocity increasing. This behavior as applied for path material and plane stress and plane strain.
8. The strain energy method is applied for all velocity impact and gives good agreement when velocity impact increasing more than 20 m/s. Where the percentage error for result between the airy method and energy about (13%).
9. Possibility of using the neutral frequency of plate without crack result for plate with crack when the $\left(c_o/A\right) < 0.03$ for isotropy material. Where the percentage error is lowest than (4%).
10. The dynamic normalized stress intensity factor is depended on the geometry of model and dimension of crack. Also when the deep of crack is increasing the factor is increasing this meaning the crack growth possibility effective.

***(5) Z.Y. Zhang and M.O.W. Richardson(2007)*[17]**, investigated low velocity impact induced non-penetration damage in pultruded glass fiber reinforced polyester (GRP) composite materials using an instrumented falling weight impact test machine with a chisel shaped impactor. The characteristics of the impact event, force/time and force/deflection traces were determined. The internal damage was visualized and quantified by Electronic Speckle Pattern Interferometry (ESPI) in terms of the thickness, density and uniformity degradations of fringe patterns. There is a linear relationship between the impact energy and the identified damage areas. The post impact structural integrity of impacted specimens was evaluated by three point bending tests. It reveals that there is a significant reduction in flexural properties due to the impact-induced damage and that the residual flexural strength is more susceptible to damage than residual modulus.

2-4 Dynamic Crack Growth(DCG):

(1) Alan T. Zehnder, et al.(1999) **[18],** studied Analytically in shell structures subjected to very complex stress states. Using small deflection Kirchoff plate theory to calculate stress at the crack tip and crack growth to compare with (F.E.M.) and experimental results, they showed that crack growth is not dependent on mode I only, but depend on a combination of parameters. The shear loads induces a great deal of contact and friction on the crack surfaces dramatically reducing crack growth rate.

(2) M. J. Maleski et al (2002) **[19],** They represented experimental technique for measuring crack tip and Dynamic Stress Intensity Factors (DSIFs) and compared with numerical and analytical solutions. The method exploits optimal positioning of stacked strain gage rosette near the crack tip, the method is demonstrated for quasi-static, low velocity impact loading condition and two values of crack length to plate width ratio. They noted that experimental results are good agreement with those obtained from numerical simulations.

*(3) Yung-Tze Chen,(2003)***[20]**, studied the crack propagation of linear elastic cracked plates .An analytical solution for crack propagation of the cracked plates subjected to uniform static loading with simply supported boundary conditions is developed by means of Galerkin method coupled with integral transform method.

Results for this analyses are used to draw conclusion regarding the ability of relating crack speed ratios to aspect ratio, to crack length ratio, and the stress intensity factor.

The rational approach for crack propagation of an elastic ,isotropic, homogeneous rectangular plate with full in depth crack has been proposed with success by means of Galerkin method coupled with integral transform method. He conclude that ,the stress intensity factor ratios decrease in sinusoidal fashion with increasing crack length ratios and inversely decrease as crack-speed ratios are increased.

***(4) Seung Jo Kim, Nam Seo Goo & Tae Won Kim,* (1997)[21],** investigated the dynamic behavior and impact-induced damage of laminated composite structures. Special attention is given to curved structures, which have been widely used in various aerospace applications. A three-dimensional finite-element code is developed that can describe dynamic and impact behavior and predict the impact-induced damage of shell-shaped structures. Incompatible eight-nodded brick elements with Taylor's modification and a successive coordinate transformation scheme are adopted. A modified Hertzian contact law is utilized to compute the contact force for an isotropic sphere on a cylindrical composite shell. The governing equation is integrated in time by the Newmark method. A scheme of detection of impact-induced damage is proposed for determining damage patterns resulting from low-velocity impact.

The parametric study of the dynamic behavior of cylindrical composite shells with various curvatures and stacking sequences is presented. The results are compared with those of plates of the same dimensions and stacking sequences. As the curvature increases, the maximum impact force becomes higher for the same impact velocity. Although the delamination patterns of the cylindrical shell have a similar tendency to those of the plates, the delaminated area widens as the curvature increases

At this study curved plate analyses of deflection, stress and dynamic crack growth analytically derived using classical method and by both energy and classical methods as well as the finite element method of analyzing using ANSYS10 program under the action of direct compression in x-direction ,shear force in the plane of the panel and low velocity impact with different velocities located at the center of the panel, FORTRAN90 programming language has been used to find the values of the equations derived in this study, ANSYS10 finite element program and other methods (classical and energy) are used to analyze the same problem to compare the results achieved by them.

The stresses ,deflection and dynamic crack growth can be calculated for different thickness, velocities, time duration of impact ,and various radii of curvature in x-z and y-z planes, different aspect ratios and variable values of direct compression and shear force can be apply using the same program also another location of impact can be analyzed.

Chapter Three

Analytical Solution

CHPTER THREE

ANLYTICAL SOLUTION

3-1 Introduction

This study will concentrate on analyzing deflection, principal stresses, in-plane stress intensity factors(KI and KII) using different methods (classical, energy and finite element using ANSYS 10 program).

The panel will considered as curved type i.e. has initial deflection with magnitude depend on the radius of curvature and the plane at which it lies. The panel subjected to in-plane forces(direct compression and shear) and out of plane load (low velocity impact by spherical impactor).

Figure(3-1) shows the general shape of the panel under the action of all loads under consideration. All edges of the panel will be consider as simply supported.

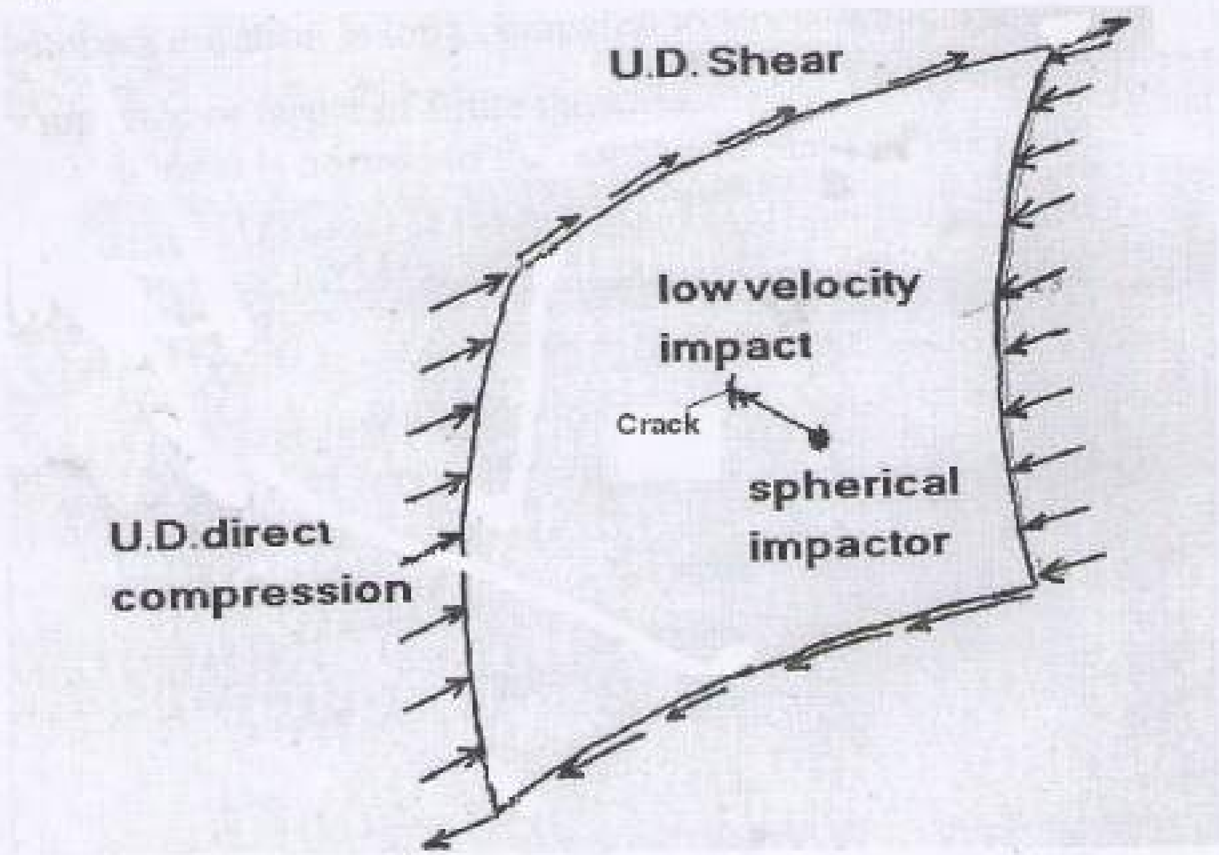

Figure(3-1) Shape of panel under loading system (case study).

3-2 Assumptions

To get the analytical solution using plate theory the following assumptions will be considered:

1-The material of plate is elastic, homogeneous & isotropic.

2- The plate has initial curvature i.e. initial deflection (w_o), as shown in Figure (3-2).

3- The deflection of the mid-plane is small compared with thickness of the plate ,so the square of the slope can be neglected.

4- The straight lines initially normal to the mid-plane stay straight and normal during deformation.

5-The stress normal to the mid-plane oz is small compared with the other stress component and may be neglected .

6-The middle surface remain unstrained after bending (i.e. neutral axis coincide with the mid plane.

For low velocity impact the vibration effect can be safely neglected,**[22]** and the following assumption will be considered:

7-The target and the impactor are linear elastic.

8-Impact duration is long compared to stress-wave transient time in the impactor or target of finite thickness.

9-The impact is normal to the target mid plane of the panel.

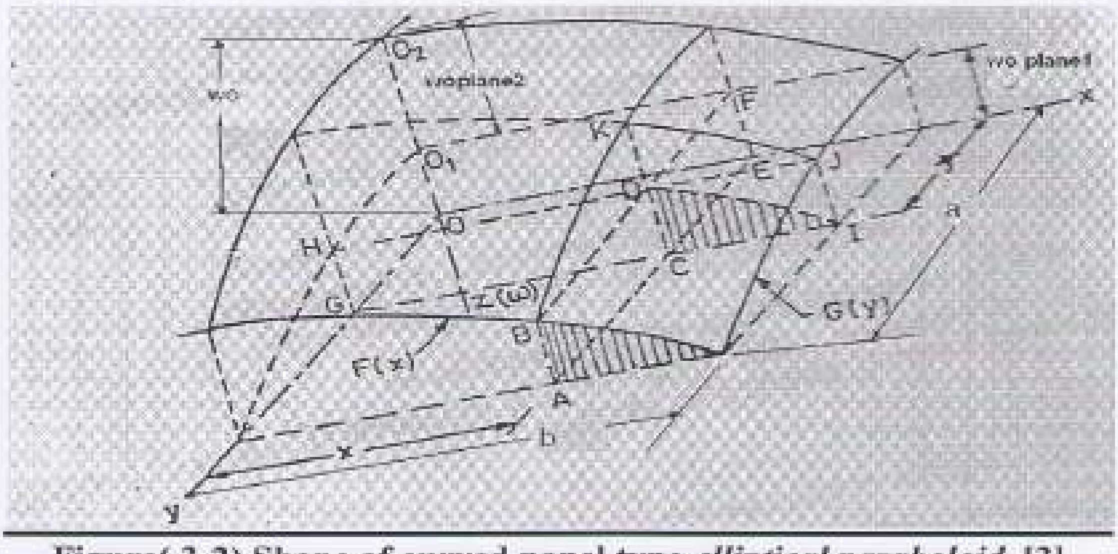

Figure(3-2) Shape of curved panel type *elliptical paraboloid* .[3]

3-3 Boundary Conditions:

For all edges simply supported we have

$w = 0 \mid_{x=0,a}$

$w = 0 \mid_{y=0,b}$

$$M_x = -D\left(\frac{\partial^2 w}{\partial x^2} + \mu\frac{\partial^2 w}{\partial y^2}\right) = 0$$

$$M_y = -D\left(\frac{\partial^2 w}{\partial y^2} + \mu\frac{\partial^2 w}{\partial x^2}\right) = 0$$

Where

$$D = \frac{Eh^3}{12(1-\mu^2)} = \textit{the lateral rigidity of the plate} \text{ ....(3.1)}$$

And

h: the plate thickness.

E: Modulus of elasticity.

μ: poisons ratio.

3-4 Governing Equation for Deflection of Plates in Cartesian Coordinate:

The general governing equation for deflection of plates in Cartesian coordinate subjected to lateral load (p) can be written as,[3]:

$$\nabla^4 w = \frac{p}{D} \qquad \text{..(3.2)}$$

Where

p is the lateral force(i.e. the pressure due to impact).

and

$$\nabla^4(\,) = \frac{\partial^4 w}{\partial x^4} + \frac{\partial^4 w}{\partial x^2 \partial y^2} + \frac{\partial^4 w}{\partial y^4} \qquad \text{..................................(3.3)}$$

And for lateral and in-plane forces the general equation will be, [7] :

$$\nabla^4 w = \frac{1}{D}\left(p + N_x\frac{\partial^2 w}{\partial x^2} + 2N_{xy}\frac{\partial^2 w}{\partial x \partial y} + N_y\frac{\partial^2 w}{\partial y^2}\right) \text{ ....(3.4)}$$

Where

p =the lateral load (impact load).

N_x = direct compression/tension force in x-direction.

N_y = direct compression/tension force in y-direction.

N_{xy} = shear force in xy-plane.

Let now consider a plate with an initial deflection w_0 (i.e. curved plate) .It is assumed that : w_0 is small compared with the plate dimensions .If the plate is subject to in plane and lateral loads then an additional deflection w_1 occurs and the total deflection is,[7]:

$$w = w_o + w_1 \quad \ldots\ldots\ldots\ldots\ldots\ldots\ldots\ldots\ldots\ldots\ldots\ldots\ldots\ldots (3.5)$$

Here w_1 is the solution of eq.(3.2). If beside the lateral load , the direct forces are also applied to an initially curved plate, then these forces produce bending , which depends not only on w_1 but also on w_o , in order to determine the total deflection w let introduce eq.(3.5) in to the right hand of eq.(3.4).

The left-hand side of this equation takes into account a change in curvature from the initial curved state due to a given lateral load . Therefore w_1 has to be substituted for (w) on the left-hand side of equation (3.4), for the initially curved plate the governing equation will be of the following form,[7]:

$$\nabla^4 w_1 = \frac{1}{D}\left(p + N_x \frac{\partial^2(w_1+w_o)}{\partial x^2} + 2N_{xy}\frac{\partial^2(w_1+w_o)}{\partial x \partial y} + N_y \frac{\partial^2(w_1+w_o)}{\partial x^2}\right) \ldots\ldots (3.6)$$

As mentioned previously , the influence of the initial curvature on the total deflection of the plate is equivalent to the influence of some fictitious lateral load of intensity p_f expressed as,[7]:

$$p_f = N_x \frac{\partial^2 w_o}{\partial x^2} + N_y \frac{\partial^2 w_o}{\partial y^2} + 2N_{xy}\frac{\partial^2 w_o}{\partial x \partial y} \quad \ldots\ldots\ldots\ldots\ldots\ldots\ldots\ldots\ldots (3.7)$$

For the case under study the lateral load will be the impact load which is a function of *time* and *the coordinate of the contact region.*

3-5 Geometry of the Curved Plate

Curved plates have an initial deflection depend on the radius of curvature and the type of the curved plate. The case of study has double curvature panel, this type named *elliptical paraboloid* , the trigonometric relations gives the value of that initial deflection,**[3]**.

When there are more than one radius of curvature as in the case under study which has a double curved shape (i.e. in x-z plane and y-z plane) as shown in Figure(3.2) which refers clearly to that: The total initial deflection is the sum of the initial deflection of the first plane and that of the second one.

The length of the arc is known according to the dimension of the plate under study, so

$\rho_1\varphi$=length of arc.

where

ρ_1=radius of curvature in plane 1(i.e. curvature in xz plane).

φ=centric angle of the arc in that plane.

The initial deflection (w_o) will be

$$(w_o)_{plane1} = \rho_1\left(1-\cos\left(\frac{\varphi}{2}\right)\right) \quad \text{.........................(3.8)}$$

By the same way for the other plane

$$(w_o)_{plane2} = \rho_2\left(1-\cos\left(\frac{\beta}{2}\right)\right) \quad \text{.........................(3.9)}$$

where

ρ_2=radius of curvature in plane 2(i.e. curvature in yz plane).

ß=centric angle of the arc in that plane.

The total initial deflection will be

$$w_o = (w_o)_{plane1} + (w_o)_{plane2} \quad \text{............................(3.10)}$$

3-6 Curvature Parameter (Zp):

When the radius of curvature varies the mode of loading and the stresses induce in the plate also changed ,the critical stresses (bending & shear) and buckling load also change .The method of fixing the ends of the panel play great effect , the shear and compressive buckling parameters also changed (many books gives the relation between shear and compressive parameters and the curvature parameter).

The curvature parameter represented as **[9]**:

$$z_{p_1} = \frac{B^2}{\rho_1 h}(1-\mu^2) \quad \text{...(3.11)}$$

Where:

B :Length of the shorter side of the plate.

For the case under study there are two radiuses of curvature and the effective curvature parameter can be calculated as **[23]** :

$$Z_p = \frac{1}{\left(\frac{1}{z_{p1}}\right)+\left(\frac{1}{z_{p2}}\right)} \quad \text{...(3.12)}$$

Where z_{p1} = curvature parameter of first curved (i.e. x-z plane).

z_{p2} = curvature parameter of second curved (i.e. y-z plane).

3-7 Buckling of Plates:

When plates subject to large in plane loads either compressive or shear ,they buckle. The buckling phenomena is not linear because it characterized by disproportional increase of the displacement associated with the small increment of the loads,**[3]**.

In plates ,buckling may be due to the action of in-plane normal forces (Nx and Ny) along x and y direction respectively or due to shear forces (Nxy) in the *xy* plane, either acting individually or as a combination.

Unlike columns, the plate failure does not occur when the critical buckling load is reached .Plates continue to resist the in-plane loads far in excess to the critical load before failure ,thus the post buckling behavior of plates plays an important role in determining the ultimate carrying capacity,[24].

Consider a rectangular infinite small element dx×dy has been bent under the in-plane forces Nx ,Ny ,Nxy ,Nyx , and transverse forces/moment Mx ,My ,Mxy ,Myx ,Qx ,Qy will be as shown in Figure (3-3).

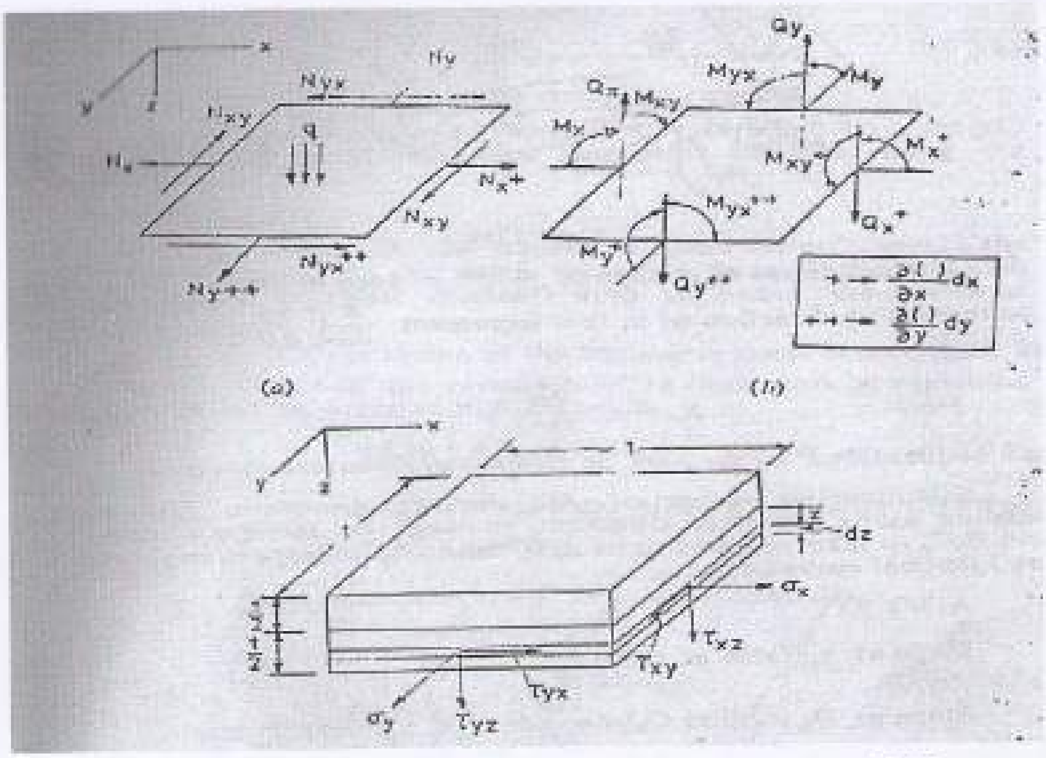

Figure(3-3) External loads can applied on a panel,[3].

Let the internal resistive force appears as in-plane forces applied on the element (per unit length of the side on which they act) ,remembering that for large deflection of plates there are in-plane forces in addition to the transverse moments and shear.

For transverse moments and shear

$$\nabla^4 w = 0$$

The equilibrium differential equation due to lateral and in-plane will be as,**[7]**:

$$\nabla^4 w_1 = \frac{1}{D}\left(p + N_x \frac{\partial^2 (w_t)}{\partial x^2} + 2N_{xy}\frac{\partial^2 (w_t)}{\partial x \partial y} + N_y \frac{\partial^2 (w_t)}{\partial x^2}\right) \quad .....(3.13)$$

Where

w_t =total deflection=$w_1 + w_o$

For the case under study Ny=o

p: is the impact load.

N_{xy}:Shear force applied in xy plane.

Buckling parameter is one of the most useful values because it describe the buckling behavior and it calculated analytically or by empirical formulas, these parameters achieved by equating the in-plane forces to zero except one then substitute the suggested equation of deflection in eq.(3.13) to find that load then derive the expression and equate the derivative to zero to find the smallest critical buckling load,(for more information see **[3]** and**[22]**).

For bending buckling produced by direct compression the values of buckling parameter for all edges simply supported with different aspect ratios are given in Table(3-1). When a panel subjects to direct compression only, the critical buckling load can be determined with a given mode & geometry as**[22]** :

$$\sigma_{cr} = \frac{K_b \pi^2 E}{12(1-\mu^2)}\left(\frac{h}{B}\right)^2 \quad ....(3.14)$$

Where :

K_b =Bending buckling stress parameter.

Table(3-1) Bending buckling parameter with aspect ratio of all edges simply supported curved plate.[9]

A/B	0.5	0.6	0.667	0.75	0.8	0.9	1.0	1.5	2.0
K_b	25.6	24.1	23.9	24.1	24.4	25.6	25.6	24.1	23.9

For other type of boundary conditions such as clamped end just the values of the bending buckling parameter will change,**[25]**.

For the case of shear force only (i.e. shear buckling), Table (3-2) shows the shear buckling parameter for all edges simply supported curved plate with different aspect ratios, and the critical shear buckling stress will be **[9]:**

$$\tau_{cr} = \frac{K_S \pi^2 E}{12(1-\mu^2)} \left(\frac{h}{B}\right)^2 \quad \ldots\ldots\ldots\ldots\ldots\ldots\ldots\ldots\ldots(3.15)$$

Where:

K_{s}= Shear buckling stress parameter.

Table(3-2) Values of shear buckling parameter (K_s) of all edges simply supported plate. [22]

A/B	1	1.2	1.4	1.5	1.6	1.8	2	2.5	3	4
K_s	9.34	8.0	7.3	7.1	7.0	6.8	6.6	6.1	5.9	5.7

When both bending and shear are applied on a plate, or there is also lateral load the principal stress (σ_1) can be used with Table(3-1) since there is no shear in the plane of principal stresses, S. P. Timoshenko **[22]** calculate the buckling parameter for combined shear and bending stresses according to the ratio of $(\frac{\sigma}{\tau})$, the critical buckling stress will be:

$$\sigma_{cr} = \frac{K_{comb} \pi^2 E}{12(1-\mu^2)} \left(\frac{h}{B}\right)^2 \quad \ldots\ldots\ldots\ldots\ldots\ldots\ldots\ldots\ldots\ldots(3.16)$$

Where

K_{comb} =buckling parameter for combined shear and direct Compression.

Table(3-3) below shows the buckling parameter for combined shear and direct compression with (aspect ratio=1)

Table (3-3) Buckling parameter of combined shear and direct compression, with aspect ratio=1.[22]

$\frac{\sigma}{\tau}$	0.0	0.5	1.0	1.5	2.0
K_{comb}	14.71	7.09	4.5	3.24	2.51

For other aspect ratios see *theory of elastic stability by Timoshenko***[22].**

3-8 Deflection and Stresses in Curved Plate

Let the initial deflection represented by the form,**[7]**:

$w_0 = \alpha_{mn} \sum_m^\infty \sum_n^\infty sin \frac{m\pi x}{A} sin \frac{n\pi y}{B}$ ....(3.17A)

α_{mn}: The initial deflection at the center of the plate.

The deflection due to apply of external force will be

$w_1 = w_{mn} \sum_m^\infty \sum_n^\infty sin \frac{m\pi x}{A} sin \frac{n\pi y}{B}$ ....(3.17B)

w_{mn} : The mode shape of deflection

Also the deflection due to direct compression only according to Navier's solution is

$w_1 = A_c \sum_m^\infty \sum_n^\infty sin \frac{m\pi x}{A} sin \frac{n\pi y}{B}$ ....(3.18)

Where

A_c = constant.

n & m: number of half sine waves of the panel shape in x and y directions resp.

Substituting in Eq.(3.6) putting N_{xy}, p *and* N_y equal to zero gives**[22]**:

$wc = \frac{\alpha_{mn}}{1-\beta} \sum_m^\infty \sum_n^\infty sin \frac{m\pi x}{A} sin \frac{n\pi y}{B}$ ....(3.19)

where

wc=deflection due to direct compression only.

$\beta = \frac{N_x}{\frac{\pi^2 D}{A^2}[1+\left(\frac{A}{B}\right)^2]^2}$ ....(3.20)

Now, to find the deflection due to shear only put N_x, p *and* N_y in Equaton (3.13) equal to zero, using

$w_s = A_s \sum_m^\infty \sum_n^\infty sin \frac{m\pi x}{A} sin \frac{n\pi y}{B}$ ....(3.21)

Where

A_s = constant.

The expression for the deflection equation under shear only will be :

$$ws = \alpha_{mn} \sum_m^{\infty} \sum_n^{\infty} \left\{ 1 + \frac{\frac{2N_{xy}}{D}}{\frac{\pi^2 (A^2+B^2)^2}{A^3 B^3} tan \frac{m\pi x}{A} tan \frac{n\pi y}{B} \frac{2N_{xy}}{D}} \right\} \{sin \frac{m\pi x}{A} sin \frac{n\pi y}{B}\} \ldots\ldots (3.22)$$

Where

w_s = The deflection due to shear only.

For more information appendix (A) contain the derivative of equations(3.19) & (3.22).

For the case of combined shear and direct compression, by adding (3.19)and (3.22) gives

$$w_{sc} = \sum_m^{\infty} \sum_n^{\infty} \alpha_{mn} [\frac{1}{1-\beta} + \left\{ 1 + \frac{\frac{2N_{xy}}{D}}{\frac{\pi^2 (A^2+B^2)^2}{A^3 B^3} tan \frac{m\pi x}{A} tan \frac{n\pi y}{B} \frac{2N_{xy}}{D}} \right\}] sin \frac{m\pi x}{A} sin \frac{n\pi y}{B}$$

$$\ldots\ldots\ldots\ldots\ldots\ldots (3.23)$$

Where

w_{sc} = Deflection due to shear and direct compression.

Attention should be taken that super position method can not apply if there is out of plane force.

3-9 Pressure Distribution Due to Impact:

Let m_{im} and v_{im} be the mass and velocity of the impactor respectively ,and the mass and velocity of the target be m_2 and v_2 respectively .The rate change of velocity during impact for the impactor and target will be according to Newton's second low as :

$$m_{im} \frac{dv_{im}}{dt} = F \quad \text{and} \quad m_2 \frac{dv_2}{dt} = F \ldots\ldots\ldots\ldots\ldots\ldots (3.24)$$

Let the distance of approach of the impactor and the target because of the local compression due to impact be α .then the velocity of approach is

$$\dot{\alpha} = v_{im} + v_2 \ldots\ldots\ldots\ldots\ldots\ldots\ldots\ldots (3.25)$$

According to Hertzian contact, **[6]**:

$p = n_c \alpha^{\frac{3}{2}}$ ....(3.26)

And $\quad n_c = \frac{4\sqrt{R_i}}{3\pi(k_1+k_2)}$ ....(3.27)

Where

R_i = Radius of aspherical impactor

$k_1 = \frac{1-\mu_1^2}{\pi E_1} \quad \& \quad k_2 = \frac{1-\mu_2^2}{\pi E_2}$ ....(3.28)

E and μ refer to modulus of elasticity and Poisson's ratio respectively. and the subscript 1 & 2 refer to impactor and the target respectively.

Differentiate (3.25) and combine with (3.24) gives,**[6]**:

$\ddot{\alpha} = n_c M_c \alpha^{\frac{3}{2}}$ ....(3.29)

Where

$M_c = \frac{1}{m_{im}} + \frac{1}{m_2}$

Multiply both side of (3.29) by $\dot{\alpha}$ and integrate to get

$\dot{\alpha}^2 - v^2 = -\frac{5}{4} M_c n \alpha^{\frac{5}{2}}$ ....(3.30)

Where

$\dot{\alpha}$:approach velocity at the beginning of the impact.

Maximum deformation α_1 occurs when $\dot{\alpha} = 0$ and

$\alpha_1 = (\frac{5 v_{im}^2}{4 M_c n_c})^{\frac{2}{5}}$ ....(3.31)

Let the impactor velocity be v_{im} ,the energy balance becomes

$\frac{1}{2} m_{im} v_{im}^2 = \int_0^{\alpha_1} p d\alpha$ ....(3.32)

Substitute p from (3.26) and integrate to get

$\frac{1}{2} m_{im} v_{im}^2 = \frac{2}{5} n_c \alpha^{5/2}$ ....(3.33)

Let $v_1 = v_{im}$ and $M_c = \frac{1}{m_{im}}$,substitute eq.(3.31) in to eq.(3.26) gives

$p = n_c{}^{2/5} [\frac{5v^2}{4M_c}]^{3/5}$ ....(3.34)

The relation between radius of hertzian contact and the pressure due to impact will be

$r_c = [\frac{3\pi p}{4}(k_1 + k_2)R_i]^{\frac{1}{3}}$ ....(3.35)

Where

r_c =radius of patch due to impact.

Substitute p from eq. (3.34) in to eq. (3.35) gives:

$r_c = (R_i)^{\frac{1}{2}}(\frac{5v_{im}^2}{4M_c n_c})^{\frac{1}{5}}$ ....(3.36)

It has been shown by (Hertz 1881) and Timoshenko (1934) that; the pressure distribution over the area of contact is**[6]**

$p_{x,y} = p_0[1 - \frac{x^2}{r_c^2} - \frac{y^2}{r_c^2}]^{\frac{1}{2}}$ ....(3.37)

Where p_0 is the maximum pressure (i.e. the pressure at the center of contact) and

$p_0 = \frac{3p}{2\pi r_c^2}$ ....(3.38)

3-10 Impact Response of Flexible Target:

For flexible plate type target , the surface pressure, area of contact and impact duration will be a function of the parameters (mass and velocity of impactor & elastic properties of the impactor and target) as well as plate bending stiffness (D) and boundary condition. For a given impact velocity the magnitude of dynamic force p will decrease as the target flexibility increase (or decrease the target thickness) , increase in target flexibility will also increase contact duration time and decrease the area of contact,**[6]**.

3-11 Impact Time Duration :

The time duration calculated by Timoshenko (1934) from the problem of impact of two bodies as,**[6]**:

$\dot{\alpha}^2 - v^2 = -\frac{4}{5}M_c n_c \alpha_1^{\frac{5}{2}}$ ....(3.39)

Or

$\dot{\alpha} = (v_{im}^2 - 4/5(\,Mn_c{\alpha_1}^{5/2}\,))^{0.5}$ ....(3.40)

Substitute $\dot{\alpha} = \frac{dx}{dt}$ and solving for (dt) gives

$dt = \frac{dx}{(v^2 - \frac{4}{5}Mn\alpha^{\frac{5}{2}})^{\frac{1}{2}}}$ ....(3.41)

Integrate to get

$t = \frac{2\alpha_1}{v}\int_0^x \frac{dx}{(1-x^{5/3})^{\frac{1}{2}}}$ ....(3.42)

Where

$x = \frac{\alpha}{\alpha_1}$

The total impact duration (t_o) is obtained by integration between the limit (x=0) and (x=1),**[6]**.

$t_0 = 2.94(\frac{5}{4M_c n_c {v_{im}}^{0.5}})^{\frac{2}{5}}$ ....(3.43)

The variation of surface pressure (p) , radius of the area of contact (r_c) and surface pressure distribution ($p_{x,y}$) with time can be determined by first numerically integrating (3.42) and determine ($\frac{\alpha}{\alpha_1}$) as a function of time ($\frac{t}{t_0}$).

The resultant plot of this solution is shown in Fig(3-4), the curve can be approximated fairly accurately by an equation:

$\alpha = \alpha_1 \sin\frac{\pi t}{t_0}$ ....(3.44)

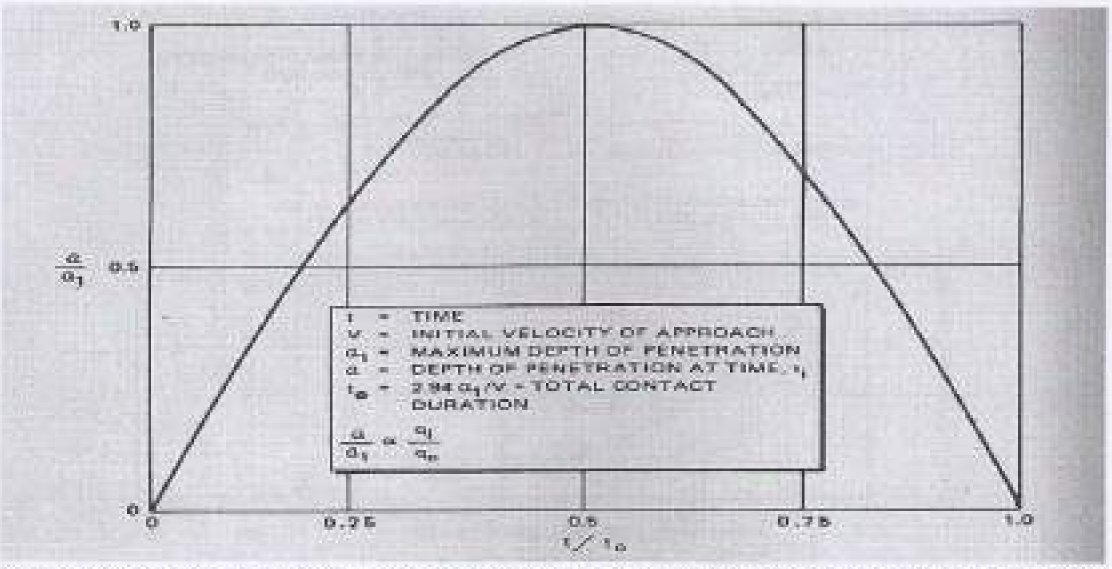

Figure(3-4) Generalized pressure-time relationship of low velocity impact.[6]

Substitute (t_0)from (3.43) gives

$$\alpha = \alpha_1 \sin\frac{\pi t v}{2.94\alpha_1} \quad \text{.......................................(3.45)}$$

From (3.26) one can get

$$p(t) = \frac{3ns}{8\pi Z_p mr}\,(\alpha_1 sin\frac{\pi t v}{2.94\alpha_1})^{\frac{1}{2}} \quad \text{..................................(3.46)}$$

The pressure distribution at the contact region will be,**[6]**:

$$p(_{u_0,v_0,}t) = p(t)\left(1-\frac{u_0{}^2}{r_c{}^2}-\frac{v_0{}^2}{r_c{}^2}\right) \quad \text{..................................(3.47)}$$

Where (u_o *and* v_o) is the width and length of the patch area produced by impact.

Substitute (3.46) in (3.47) gives

$$p(_{u_0,v_0,}t) = \frac{3n_c s}{8\pi Z_p m_c r}\,(\alpha_1 sin\frac{\pi t v}{2.94\alpha_1})^{\frac{1}{2}}\left(1-\frac{u_0{}^2}{r_c{}^2}-\frac{v_0{}^2}{r_c{}^2}\right) \quad \text{........(3.48)}$$

3-12 Influence of Target Curvature :

Target curvature effects both magnitude and distribution of surface pressure caused by impact as well as the shape of the area of contact. The influence of target curvature noted by Greszcuk and Chao (1975) are, **[13]:**

1-Area of contact is elliptical and approach circle as the radius of curvature increase.

2-The area of contact decrease with decreasing radius of curvature.

3-Maximum load resulting from impact decreases with decreasing radius of curvature.

4-Maximum surface pressure increase with decreasing radius of curvature.

5-Contact duration time increase with decreasing radius of curvature.

In the case of study there are two curvatures of the curved plate so the general contact relation should be used. Hertz showed that the intensity of pressure between the contacting surfaces could be represented by the elliptical

(or, rather, semi ellipsoid) construction shown in Fig(3-5). The total contact load is given by the volume of the semi-ellipsoid,**[23].**

$p = \frac{2}{3}\pi \mathcal{A}\mathcal{B}p_o$ ....(3.49)

Where

$\mathcal{B}$= the length of minor axis of the elliptical patch.

$\mathcal{A}$=the length of major axis of the elliptical patch.

p_o=the maximum pressure of contact.

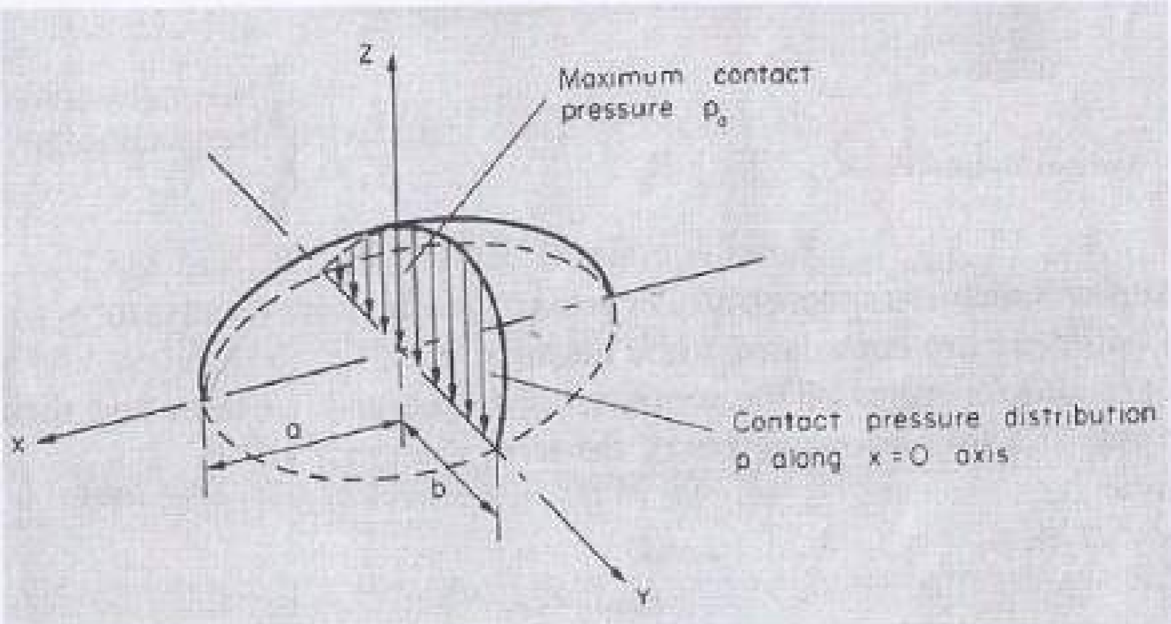

Figure(3-5) Pressure distribution between two curved bodies in contact.[23]

The maximum pressure p_o will be

$p_o = \frac{3p}{2\pi\mathcal{A}\mathcal{B}}$ ....(3.50)

$\mathcal{A} = mm[\frac{3p\Delta}{4\forall}]^{\frac{1}{3}}$ ....(3.51)

$\mathcal{B} = nn[\frac{3p\Delta}{4\forall}]^{\frac{1}{3}}$ ....(3.52)

Where

mm and nn are constants.

$\Delta = \frac{1}{E_1}[1 - \mu_{im}{}^2] + \frac{1}{E_{target}}[1 - \mu_{target}{}^2]$ ....(3.53)

$\forall = \frac{1}{2}[\frac{1}{R_l} + \frac{1}{R_{im}} + \frac{1}{\rho_1} + \frac{1}{\rho_2}]$ ....(3.54)

R_i, R_{im} =maximum and minimum radiuses of impactor respectively in unloaded contact in two perpendicular planes=R_i .

ρ_1, ρ_2 = maximum and minimum radiuses of target(plate) respectively in unloaded contact in two perpendicular planes.

Let

$$\gamma = cos^{-1}\left(\frac{Jb}{\forall}\right) \quad \ldots\ldots\ldots\ldots\ldots\ldots\ldots\ldots\ldots\ldots\ldots (3.55)$$

Where

$$Jb = \frac{1}{2}\left(\frac{1}{\rho_1} - \frac{1}{\rho_2}\right)^2 \quad \ldots\ldots\ldots\ldots\ldots\ldots\ldots\ldots\ldots\ldots\ldots (3.56)$$

Introduce two constants (mm and nn) they are also functions of the geometry of the contact surfaces and their values are shown in table(3-4) for various values of γ .

Table (3-4) Values of constants for contact of impact.[23]

γ degrees	20	30	35	40	45	50	55
mm	3.778	2.731	2.397	2.136	1.926	1.754	1.611
nn	0.408	0.493	0.530	0.567	0.604	0.641	0.678

γ degrees	60	65	70	75	80	85	90
mm	1.486	1.378	1.284	1.202	1.128	1.061	1.00
nn	0.717	0.759	0.802	0.846	0.893	0.944	1.00

* mm and nn are constants.

3-13 Conversion of Elliptical Patch to Rectangular :

In finite element analysis stress modeling of circular area is much difficult than from the rectangular one. According to Timoshenko**[25]**, acicular and a square loaded area are equivalent with respect to the bending moments they produce at the center of the area ,if :

$$\mathcal{A} = \frac{u_o}{\sqrt{2}} e^{\frac{\pi}{4}-1} = 0.57u_o \quad \text{or} \quad u_o = 0.88 * 2\mathcal{A} \quad \ldots\ldots\ldots\ldots (3.57)$$

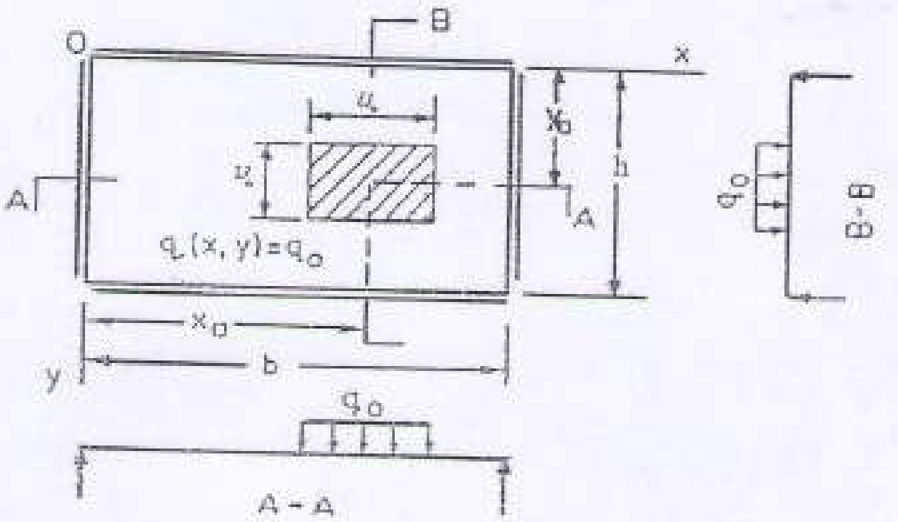

Figure(3-6) Conversion of elliptical contact patch to rectangular.[15]

$v_o = 0.88 * 2B$ ....(3.58)

Where (u_o *and* v_o) is the width and length of the patch area produced by impact.

3-14 Deflection Due to Impact, Shear, and Direct Compression

The deflection due to impact only can be expresses as,[7]and,[22]:

$$w_i = \frac{16p(t)}{\pi^6 D} \sum_m^\infty \sum_n^\infty \frac{s_{mn} \sin\frac{m\pi x}{A} \sin\frac{n\pi y}{B}}{mn(\frac{m^2}{A^2}+\frac{n^2}{B^2})^2} \quad ....(3.59)$$

Where:

$$s_{mn} = \sin\frac{m\pi\zeta}{a} \sin\frac{n\pi\eta}{b} \sin\frac{m\pi u_o}{2a} \sin\frac{n\pi v_o}{2b}] \quad ....(3.60)$$

Where

ζ & η the coordinates of impact location in x and y direction respectively.

u_o & v_o the dimensions of rectangular contact patch in x and y direction respectively.

For the case of impact and direct compression (i.e. lateral and in-plane forces) the deflection can be expressed as,[24]:

$$w_{ic} = \frac{16p_o(t)}{\pi^6 D}\sum_m^\infty\sum_n^\infty \frac{s_{mn}\sin\frac{m\pi x}{A}\sin\frac{n\pi y}{B}}{mn\{(\frac{m^2}{A^2}+\frac{n^2}{B^2})^2+\frac{N_x}{D}(\frac{m}{\pi A})^2\}} \quad \ldots\ldots\ldots\ldots\ldots(3.61)$$

The positive sign in front of the direct compression(N_x) will be negative because the above equation for tensile and impact, and the tensile try to reduce deflection while the direct compression increase deflection, so rewrite Eq.(3.61)as:

$$w_{ic} = \frac{16p_o(t)}{\pi^6 D}\sum_m^\infty\sum_n^\infty \frac{s_{mn}\sin\frac{m\pi x}{A}\sin\frac{n\pi y}{B}}{mn\{(\frac{m^2}{A^2}+\frac{n^2}{B^2})^2-\frac{N_x}{D}(\frac{m}{\pi A})^2\}} \quad \ldots\ldots\ldots\ldots\ldots\ldots\ldots\ldots\ldots(3.62)$$

Now ,adding the shear effect to this equation using eq.(3.6) and put (p,N_x *and* N_{xy}) not equal to zero and substitute (w_1 *and* w_o) from eq.(3.17) and eq.(3.18) respectively to get, **[27]** :

$$w_{mn} = \frac{16q_{mn}}{D\pi^6 mn\left[\left\{\left(\frac{m^2}{A^2}\right)+\left(\frac{n^2}{B^2}\right)\right\}^2+\frac{N_x m^2}{\pi^2 DA^2}+\frac{N_y n^2}{\pi^2 DB^2}+2\frac{N_{xy}mn}{\pi^2 DAB}\right]} \quad \ldots\ldots\ldots\ldots\ldots\ldots\ldots(3.63)$$

Put($N_y = 0$) in the above equation to get

$$w_{ics} = \frac{16p_o(t)}{\pi^6 D}\sum_m^\infty\sum_n^\infty \frac{s_{mn}\sin\frac{m\pi x}{A}\sin\frac{n\pi y}{B}}{mn\{(\frac{m^2}{A^2}+\frac{n^2}{B^2})^2-\frac{N_x}{D}(\frac{m}{\pi A})^2-2\frac{N_{xy}}{D\pi^2}(\frac{mn}{AB})\ \}} \quad \ldots\ldots\ldots\ldots\ldots(3.64)$$

The direction in shear force and hence shear stress has no effect but the use of negative sign here because shear force try to increase the initial deflection (i.e. the initial deflection has no possibility to decrease),the effect of pressure here is determined as uniform distributed pressure over all the plate but in the case of study the pressure due to impact is function of time, also there is an elliptical contact patch converted to patch of dimensions ($u_o * v_o$)as shown in

Fig.(3-5),also there is an initial deflection which will be increase or decrease according to the direction of impact, the initial deflection from eq.(3.17) also used, the final equation of representing the deflection in case of study will be:(see appendix A)

$$w_{ics} = w_o + \frac{16p(t)}{\pi^6 D}\sum_m^\infty\sum_n^\infty \frac{\sin\frac{m\pi\zeta}{a}\sin\frac{n\pi\eta}{b}\sin\frac{m\pi uo}{A}\sin\frac{n\pi vo}{B}\sin\frac{m\pi x}{A}\sin\frac{n\pi y}{B}}{mn\{(\frac{m^2}{A^2}+\frac{n^2}{B^2})^2-\frac{N_x}{D}(\frac{m}{\pi A})^2-2\frac{N_{xy}}{D\pi^2}(\frac{mn}{AB})\ \}} \quad \ldots\ldots.(3.65)$$

The pressure due to impact can be expressed as,**[6]**:

$$p(t) = \frac{3ns}{8\pi Z_p mr}\left(\alpha_1 sin\frac{\pi tv}{2.94\alpha_1}\right)^{\frac{1}{2}} \quad ....(3.66)$$

Now substitute w_o from eq.(3.17) in eq.(3.65) to get:

$$w_{ics} = [\alpha_{mn} + \frac{16p(t)}{\pi^6 D}\sum_m^\infty\sum_n^\infty \frac{\sin\frac{m\pi\xi}{a}\sin\frac{n\pi\eta}{b}sin\frac{m\pi uo}{A}sin\frac{n\pi vo}{B}}{mn\{(\frac{m^2}{A^2}+\frac{n^2}{B^2})^2-\frac{N_x}{D}\left(\frac{m}{\pi A}\right)^2-2\frac{N_{xy}}{D\pi^2}\left(\frac{mn}{AB}\right)\}}](sin\frac{m\pi x}{A}sin\frac{n\pi y}{B})$$

$$..........(3.67)$$

3-15 Stresses Due to Impact, Shear and Direct Compression

Stresses are function of the deflection and the following formulas can be used

$$\sigma_x = \frac{Ez}{(1-\mu^2)}\{\frac{\partial^2 w}{\partial x^2} + \mu\frac{\partial^2 w}{\partial y^2}\} \quad ....(3.68A)$$

$$\sigma_y = \frac{Ez}{(1-\mu^2)}\{\frac{\partial^2 w}{\partial y^2} + \mu\frac{\partial^2 w}{\partial x^2}\} \quad ....(3.68B)$$

$$\tau_{xy} = \frac{Ez}{(1+\mu)}\{\frac{\partial^2 w}{\partial x\,\partial y}\} \quad ....(3.68C)$$

$$\frac{\partial^2 w}{\partial x^2} = (\frac{m\pi}{A})^2[\alpha_{mn} + \frac{16p(t)}{\pi^6 D}\sum_m^\infty\sum_n^\infty \frac{\sin\frac{m\pi\xi}{a}\sin\frac{n\pi\eta}{b}sin\frac{m\pi uo}{A}sin\frac{n\pi vo}{B}}{mn\{(\frac{m^2}{A^2}+\frac{n^2}{B^2})^2-\frac{N_x}{D}\left(\frac{m}{\pi A}\right)^2-2\frac{N_{xy}}{D\pi^2}\left(\frac{mn}{AB}\right)\}}]\ (sin\frac{m\pi x}{A}sin\frac{n\pi y}{B})$$

$$....................(3.69)$$

$$\frac{\partial^2 w}{\partial y^2} = (\frac{n\pi}{B})^2[\alpha_{mn} + \frac{16p(t)}{\pi^6 D}\sum_m^\infty\sum_n^\infty \frac{\sin\frac{m\pi\xi}{a}\sin\frac{n\pi\eta}{b}sin\frac{m\pi uo}{A}sin\frac{n\pi vo}{B}}{mn\{(\frac{m^2}{A^2}+\frac{n^2}{B^2})^2-\frac{N_x}{D}\left(\frac{m}{\pi A}\right)^2-2\frac{N_{xy}}{D\pi^2}\left(\frac{mn}{AB}\right)\}}]\ (sin\frac{m\pi x}{A}sin\frac{n\pi y}{B})$$

$$..................(3.70)$$

$$\frac{\partial^2 w}{\partial x\partial y} = (\frac{mn}{AB})\pi^2[\alpha_{mn} + \frac{16p(t)}{\pi^6 D}\sum_m^\infty\sum_n^\infty \frac{\sin\frac{m\pi\xi}{a}\sin\frac{n\pi\eta}{b}sin\frac{m\pi uo}{A}sin\frac{n\pi vo}{B}}{mn\{(\frac{m^2}{A^2}+\frac{n^2}{B^2})^2-\frac{N_x}{D}\left(\frac{m}{\pi A}\right)^2-2\frac{N_{xy}}{D\pi^2}\left(\frac{mn}{AB}\right)\}}]\ (cos\frac{m\pi x}{A}cos\frac{n\pi y}{B})$$

$$....................(3.71)$$

Maximum stresses induced at the surface of the plate where $(z = \frac{H}{2})$, so

$$\sigma_x = \pi^2\frac{EH}{2(1-\mu^2)}\{\left(\frac{m}{A}\right)^2 + \mu\left(\frac{n}{B}\right)^2\}[\alpha_{mn} +$$

$$\frac{16p(t)}{\pi^6 D}\sum_m^\infty\sum_n^\infty \frac{\sin\frac{m\pi\xi}{a}\sin\frac{n\pi\eta}{b}sin\frac{m\pi uo}{A}sin\frac{n\pi vo}{B}}{mn\{(\frac{m^2}{A^2}+\frac{n^2}{B^2})^2-\frac{N_x}{D}\left(\frac{m}{\pi A}\right)^2-2\frac{N_{xy}}{D\pi^2}\left(\frac{mn}{AB}\right)\}}]\ (sin\frac{m\pi x}{A}sin\frac{n\pi y}{B})\ ....(3.72)$$

$$\sigma_y = \pi^2 \frac{EH}{2(1-\mu^2)}\{\left(\frac{n}{B}\right)^2 + \mu\left(\frac{m}{A}\right)^2\}[\alpha_{mn} +$$

$$\frac{16p(t)}{\pi^6 D}\sum_m^\infty\sum_n^\infty \frac{\sin\frac{m\pi\zeta}{a}\sin\frac{n\pi\eta}{b}sin\frac{m\pi uo}{A}sin\frac{n\pi vo}{B}}{mn\{(\frac{m^2}{A^2}+\frac{n^2}{B^2})^2-\frac{N_x}{D}\left(\frac{m}{\pi A}\right)^2-2\frac{N_{xy}}{D\pi^2}\left(\frac{mn}{AB}\right)\}}]\ (sin\frac{m\pi x}{A}sin\frac{n\pi y}{B}) \quad ......(3.73)$$

$$\tau_{xy} = \pi^2 \frac{EH}{2(1+\mu)}\{\frac{mn}{AB}\}[\alpha_{mn} +$$

$$\frac{16p(t)}{\pi^6 D}\sum_m^\infty\sum_n^\infty \frac{\sin\frac{m\pi\zeta}{a}\sin\frac{n\pi\eta}{b}sin\frac{m\pi uo}{A}sin\frac{n\pi vo}{B}}{mn\{(\frac{m^2}{A^2}+\frac{n^2}{B^2})^2-\frac{N_x}{D}\left(\frac{m}{\pi A}\right)^2-2\frac{N_{xy}}{D\pi^2}\left(\frac{mn}{AB}\right)\}}]\ (cos\frac{m\pi x}{A}cos\frac{n\pi y}{B}) \quad .....(3.74)$$

Substitute $p(t)$ from eq.(3.66), the above stresses equations can be written as:

$$\sigma_x = \pi^2 \frac{EH}{2(1-\mu^2)}\sum\ \sum\ \{\left(\frac{m}{A}\right)^2 + \mu\left(\frac{n}{B}\right)^2\}\{\alpha_{mn} + \frac{6\frac{n_c s}{\pi Z_p m_c r}(\alpha_1 sin\frac{\pi t v}{2.94\alpha_1})^{\frac{1}{2}}}{\pi^6 D}$$

$$[\frac{\sin\frac{m\pi\zeta}{a}\sin\frac{n\pi\eta}{b}sin\frac{m\pi uo}{A}sin\frac{n\pi vo}{B}}{mn\{(\frac{m^2}{A^2}+\frac{n^2}{B^2})^2-\frac{N_x}{D}\left(\frac{m}{\pi A}\right)^2-2\frac{N_{xy}}{D\pi^2}\left(\frac{mn}{AB}\right)\}}]\}\ (sin\frac{m\pi x}{A}sin\frac{n\pi y}{B}) \quad ....(3.75)$$

$$\sigma_y = \pi^2 \frac{EH}{2(1-\mu^2)}\sum\ \sum\ \{\left(\frac{n}{B}\right)^2 + \mu\left(\frac{m}{A}\right)^2\}\{\alpha_{mn} + \frac{6\frac{n_c s}{\pi Z_p m_c r}(\alpha_1 sin\frac{\pi t v}{2.94\alpha_1})^{\frac{1}{2}}}{\pi^6 D}$$

$$[\frac{\sin\frac{m\pi\zeta}{a}\sin\frac{n\pi\eta}{b}sin\frac{m\pi uo}{A}sin\frac{n\pi vo}{B}}{mn\{(\frac{m^2}{A^2}+\frac{n^2}{B^2})^2-\frac{N_x}{D}\left(\frac{m}{\pi A}\right)^2-2\frac{N_{xy}}{D\pi^2}\left(\frac{mn}{AB}\right)\}}]\}\ (sin\frac{m\pi x}{A}sin\frac{n\pi y}{B}) \quad ....(3.76)$$

$$\tau_{xy} = \pi^2 \frac{EH}{2(1+\mu)}\sum\ \sum\ \{\frac{mn}{AB}\}\{\alpha_{mn} + \frac{6\frac{n_c s}{\pi Z_p m_c r}(\alpha_1 sin\frac{\pi t v}{2.94\alpha_1})^{\frac{1}{2}}}{\pi^6 D}$$

$$[\frac{\sin\frac{m\pi\zeta}{a}\sin\frac{n\pi\eta}{b}sin\frac{m\pi uo}{A}sin\frac{n\pi vo}{B}}{mn\{(\frac{m^2}{A^2}+\frac{n^2}{B^2})^2-\frac{N_x}{D}\left(\frac{m}{\pi A}\right)^2-2\frac{N_{xy}}{D\pi^2}\left(\frac{mn}{AB}\right)\}}]\}\ (cos\frac{m\pi x}{A}cos\frac{n\pi y}{B}) \quad ....(3.77)$$

The principal stresses can be calculated for various times:

$$\sigma_1 = \frac{\sigma_x+\sigma_y}{2} + \sqrt{\{\frac{\sigma_y-\sigma_x}{2}\}^2 + \tau_{xy}^2} \quad \text{.......(3.78A)}$$

$$\sigma_2 = \frac{\sigma_x+\sigma_y}{2} - \sqrt{\{\frac{\sigma_y-\sigma_x}{2}\}^2 + \tau_{xy}^2} \quad \text{.......(3.78B)}$$

$$\theta_p = \frac{1}{2} arctan \frac{\tau_{xy}}{(\frac{\sigma_y-\sigma_x}{2})} \quad \text{.......(3.78C)}$$

Where (θ_p) angle of principal stress.

3-16 Fracture Control:

Establishment of a fracture control plan requires knowledge of two objectives namely to determine:

-The effect of cracks on strength.

-The crack growth as a function of time.

The effect of crack size on strength can be shown in Fig(3-7).

In fracture mechanics crack size is generally denoted as a, the strength is expressed in terms of the load (p). suppose a structure has no significant defects (a=0) then the strength of the structure (P_u) the ultimate design strength load.

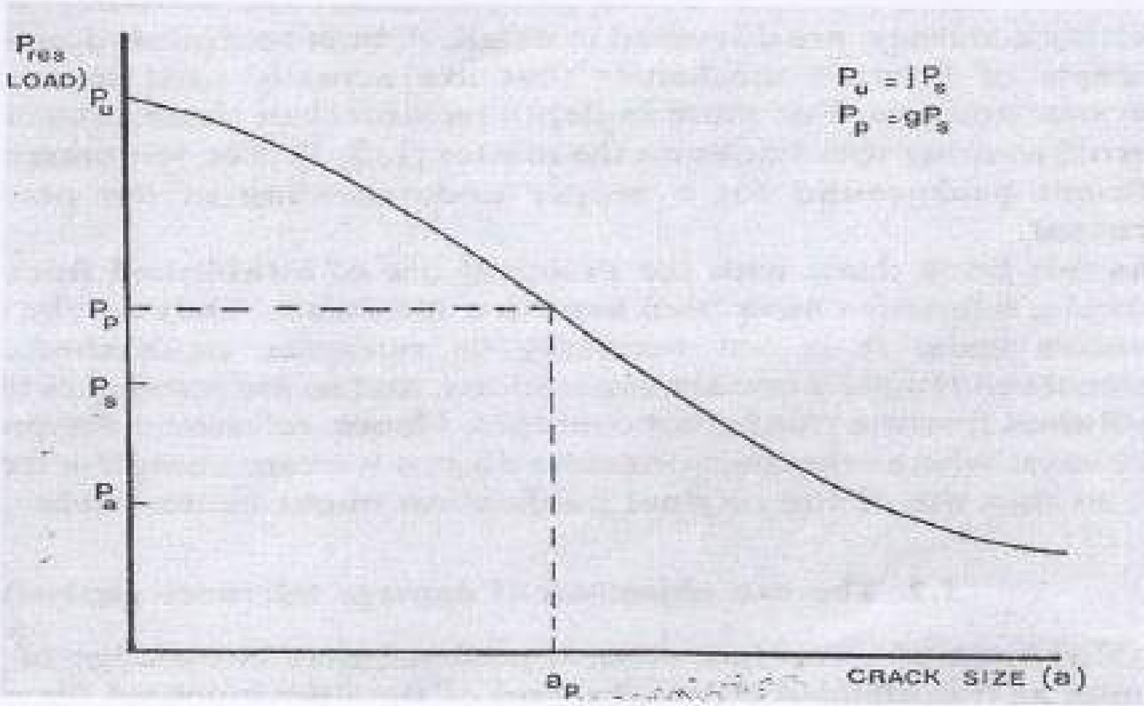

Figure(3-7) Effect of crack length on the fracture load.[2]

Strength under the presence of crack is generally referred to as the (residual strength) (P_{res}); the diagram in fig(3-6) is called the residual strength diagram .

The whole process of stable- unstable fracture may take place in a fraction of second, If the load ($P = P_{res}$) , service loading continuing at loads at or below (P_{res}) , the crack will continue to grow not by fracture but by cracking mechanisms such as fatigue , stress-corrosion or creep.

Due to continual growth the crack becomes longer , the residual strength less, the safety factor lower, and probability of fracture higher .

Starting at some crack size (a_0) the crack grows in size during time . the permissible crack(a_p) following from figure above can be plotted on the curve of crack-time variation shown in Fig(3-8) the time (H) in this figure is the safe operation time and can be determined (i.e. until (a_p) is reached).

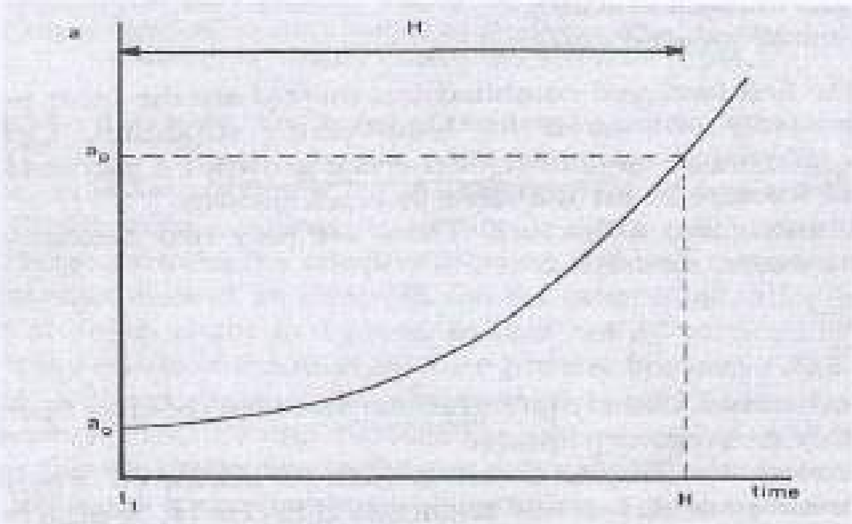

Figure(3-8) Dynamic crack growth curve (schematically).[2]

3-17 Dynamic Crack Growth and Fracture:

The residual strength and crack growth diagrams are essentially different, not only in shape but also in significance. Crack growth occurs slowly while fracture taking place very rapidly, also the mechanism of crack growth and fracture are different, there are five main type of crack growth mechanism which are:

a-fatigue due to cyclic loading.

b-stress corrosion due to sustained loading.

c-creep.

d-hydrogen induced cracking.

e-liquid metal induced cracking.

3-18 Crack Growth(Classical Method)

Many readers have no idea about the term dynamic crack growth, they consider that growth take place only with dynamic loading, but actually any variation of crack length during any period of time can be consider as dynamic crack growth, the periods may months or till years as in creep crack growth.

There are two basic aspects of dynamic crack growth :

- Finite velocities of crack propagation.
- Crack branching.

Dynamic crack growth may be considered in terms of energy balance. This can be shown with the help of Fig(3-9).After the initiation of unstable crack extension there is an excess energy which increases during crack growth, when the crack length reaches a length a_i the total excess energy represented approximately by the shaded area, actually (G) does not increase linearly with increasing crack length. Nor is it necessarily valid that (R) remains constant during crack growth. But this approximation adequate for analysis to indicate that crack velocities are finite.

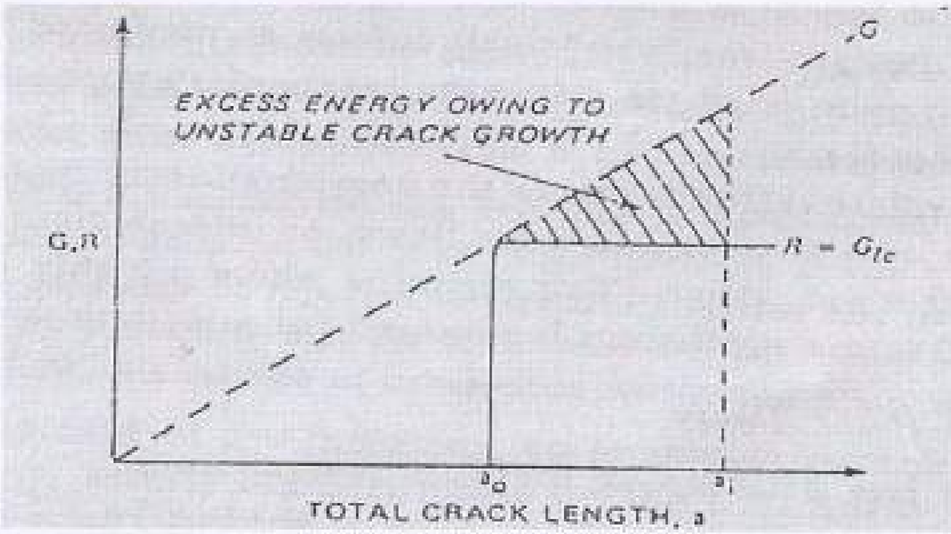

Figure(3-9) G,R-a diagram showing the excess in energy some time initiation of unstable crack extension.[1]

The excess energy can be expressed as

$$U_o = \int_{a_o}^{a_i}(G - \mathcal{R})da = -\mathcal{R}(a_i - a_o) + \int_{a_o}^{a_i}\frac{\pi\sigma^2 a}{\acute{E}}da \quad \text{........(3.79)}$$

For plane strain ($\acute{E} = E/(1-\mu^2)$) and $\mathcal{R}$ is given by

$$\mathcal{R} = \frac{\pi\sigma^2 a_o}{\acute{E}} \quad \text{..(3.80)}$$

Substitute in eq.(3.79) to get

$$U_o = -\frac{\pi\sigma^2 a_o}{\acute{E}}(a_i - a_o) + \frac{\pi\sigma^2}{2\acute{E}}(a_i^2 - a_o^2) \quad \text{....................(3.81)}$$

$$U_o = \frac{\pi\sigma^2}{2\acute{E}}(a_i - a_o)^2(a_i + a_o - 2) \quad \text{.............................(3.82)}$$

"Mott **[1]**argued that for a propagating crack the excess energy is stored as kinetic energy, a simple expression for the stored kinetic energy is obtainable from the opening displacement of the crack flank as

$$v = \frac{2\sigma}{E}\sqrt{(a_i^2 - x^2)} \quad \text{..(3.83)}$$

Since (x) is a function of (a) thus x can be written as ($x = ca$) for (0<c<1) then

$$v = \frac{2\sigma}{E}\sqrt{a_i^2(1-c^2)} = c_1\frac{\sigma a_i}{E} \quad \text{..................................(3.84)}$$

Where

$$c_1 = 2\sqrt{(1-c^2)} \quad \text{...(3.85)}$$

Since both (a_i & σ) are functions of time thus the derivative of (3.83) W.R. to time gives

$$\frac{dv}{dt} = \dot{v} = \frac{c_1}{E}(\dot{\sigma} a_i + \dot{a}_i \sigma) \quad \ldots\ldots\ldots\ldots\ldots\ldots\ldots\ldots\ldots\ldots\ldots\ldots(3.86)$$

The kinetic energy in the displaced material is:[$T=\frac{mV^2}{2}$] for a material of density (Đ) per unit thickness

$$T = \frac{1}{2} Đ.\,area.\,V^2 = \frac{1}{2} Đ \int\int (\dot{v}^2)\, dxdy \quad \ldots\ldots\ldots\ldots\ldots\ldots\ldots\ldots(3.87)$$

Substitute ($\dot{v}$) from eq.(3.86) to get

$$T = \frac{1}{2} Đ \int\int \frac{c_1^2}{E^2}(\dot{\sigma} a - \dot{a}\sigma)^2\, dxdy \quad \ldots\ldots\ldots\ldots\ldots\ldots\ldots\ldots\ldots\ldots(3.88)$$

Equating the strain energy with the kinetic energy gives:

$$\frac{\pi\sigma^2}{2E}\ (a_i - a_o)^2(a_i + a_o - 2) = \frac{1}{2} Đ \frac{c_1^2}{E^2}\int\int(\dot{\sigma} a - \dot{a}\sigma)^2\, dxdy \ldots(3.89)$$

All the Cartesian stresses (σ_x, σ_y *and* τ_{xy}) is functions of (x, y and t) so when consider only the time is variable (to find the derivative of stresses W.R.to time) these stresses can be written as:

$$\sigma_x = c_{gx}\left(sin\frac{\pi t v_{im}}{2.94\alpha_1}\right)^{0.5} \ldots\ldots\ldots\ldots\ldots\ldots\ldots\ldots\ldots\ldots\ldots\ldots(3.90A)$$

$$\sigma_y = c_{gy}\left(sin\frac{\pi t v_{im}}{2.94\alpha_1}\right)^{0.5} \ldots\ldots\ldots\ldots\ldots\ldots\ldots\ldots\ldots\ldots\ldots\ldots(3.90B)$$

$$\tau_{xy} = c_{gxy}\left(sin\frac{\pi t v_{im}}{2.94\alpha_1}\right)^{0.5} \ldots\ldots\ldots\ldots\ldots\ldots\ldots\ldots\ldots\ldots\ldots(3.90C)$$

Where

c_{gx}, c_{gy} *and* c_{gxy} are constants depend on (x, y, m, n, A, B, α_{mn}, u_o, v_o, $m_c, s, N_x, N_{xy}, n_c, z_p$) and the mechanical properties of the material of the plate (i.e. E & μ).

when derive the stresses W.R.to time to get:

$$\dot{\sigma}_x = \frac{1}{2} c_{gx}\left(\frac{\pi v_{im}}{2.94\alpha_1}\right)\frac{\cos\left(\frac{\pi t v_{im}}{2.94\alpha_1}\right)}{\left(sin\frac{\pi t v_{im}}{2.94\alpha_1}\right)^{0.5}} \quad \ldots\ldots\ldots\ldots\ldots\ldots\ldots\ldots\ldots(3.91)$$

$$\dot{\sigma}_y = \frac{1}{2} c_{gy}\left(\frac{\pi v_{im}}{2.94\alpha_1}\right)\frac{\cos\left(\frac{\pi t v_{im}}{2.94\alpha_1}\right)}{\left(sin\frac{\pi t v_{im}}{2.94\alpha_1}\right)^{0.5}} \quad \ldots\ldots\ldots\ldots\ldots\ldots\ldots\ldots\ldots(3.92)$$

$$\dot{\tau}_{xy} = \frac{1}{2} c_{gxy} \left(\frac{\pi v_{im}}{2.94 a_1}\right) \frac{\cos\left(\frac{\pi t v_{im}}{2.94 a_1}\right)}{\left(\sin \frac{\pi t v_{im}}{2.94 a_1}\right)^{0.5}} \qquad \text{.................................(3.93)}$$

Now the principal stresses variation with the time can be determined as:

$$\dot{\sigma}_1 = \frac{\dot{\sigma}_x + \dot{\sigma}_y}{2} + \sqrt{\left\{\frac{\dot{\sigma}_y - \dot{\sigma}_x}{2}\right\}^2 + \dot{\tau}_{xy}^2} \qquad \text{....................................(3.94A)}$$

$$\dot{\sigma}_2 = \frac{\dot{\sigma}_x + \dot{\sigma}_y}{2} - \sqrt{\left\{\frac{\dot{\sigma}_y - \dot{\sigma}_x}{2}\right\}^2 + \dot{\tau}_{xy}^2} \qquad \text{.................................(3.94B)}$$

The angle of the principal stresses variation with time will be:

$$\Theta_p = \frac{1}{2} arctan \frac{\dot{\tau}_{xy}}{\left(\frac{\dot{\sigma}_y - \dot{\sigma}_x}{2}\right)} \qquad \text{..(3.94C)}$$

Recall eq.(3.89), and simplify the right side to get

$$\frac{\pi \sigma^2}{2\text{Ė}} \ (a_i - a_o)^2 (a_i + a_o - 2) = \frac{1}{2} \text{Đ} \frac{c_1^2}{\dot{E}^2} \int\int (\dot{\sigma}^2 a^2 - 2\dot{a}\sigma a \dot{\sigma} + \dot{a}^2 \sigma^2) \quad \text{dxdy}$$

$$\text{.................................(3.95)}$$

Since ($\dot{a}$ *and* a) are not function of x and y and both ($\sigma^2, \dot{\sigma}\sigma$ *and* $\dot{\sigma}^2$) will be of order ($sin^2 \frac{m\pi x}{A} sin^2 \frac{n\pi y}{B}$) and the integration of them W.R.to x and y is equal to($\frac{AB}{4}$) the final result after simplifying in terms of maximum principal stress will be as :

$$\frac{4\pi\sigma^2 \text{Ė}}{\text{Đ} c_1^2} (a_i - a_o)^2 (a_i + a_o - 2) = (\dot{\sigma}^2 a^2 - 2\dot{a}\sigma a \dot{\sigma} + \dot{a}^2 \sigma^2) \quad \text{......(3.96)}$$

Solving to get ($\dot{a}$) as:

$$\dot{a}_1 = a_o \frac{\dot{\sigma}}{\sigma} + 2\sqrt{\frac{\pi \text{Ė}}{\text{Đ} c_1^2} (a_i - a_o)^2 (a_i + a_o - 2)} \quad \text{........................(3.97A)}$$